Uncertainty in Model Fitting and Simulations of a Continuously Stirred Tank Reactor (CSTR)

Jean Pierre MUHIRWA (jmuhirwa@aims.ac.tz)
AIMS141500324

African Institute for Mathematical Sciences (AIMS)

Supervised by: Prof. Tuomo KAURANNE
Lappeenranta University of Technology, Finland
Co-Supervisor: Dr. Matylda Jablonska-Sabuka
Lappeenranta University of Technology, Finland

12th July 2015

Submitted in partial fulfillment of a structured masters degree at AIMS Tanzania

Abstract

Continuously stirred tank reactors (CSTRs) play a big role in chemical engineering and in industries nowadays. Therefore, to produce quality products, it is important and necessary to make sure CSTRs work successfully by avoiding disturbance from external factors. In this work, we look at the impact of uncertainties (errors) to the model fitting and the parameter estimation of the CSTR, for both cases of exothermic and endothermic reactors. We introduced different types of noise (random noise, quasi random noise and systematic random noise) with different levels, low and high variance in the numerical solutions to generate the noisy data. Two parameters, activation energy E and reaction rate k have been estimated and investigated, due to their sensitivities to the system facilitated by the guessed noisy data and by using least square method. The results showed that, the increase of noise in measurements affects activation energy E much more than the reaction rate k for all types of noise as k converges to its true values. Also, from the results obtained, the endothermic CSTR is more sensitive than the exothermic CSTR for any kind of noise according to much deviation observed in its estimated activation energy values. Furthermore, quasi random noise has provided closer values for parameter estimation compared to the other types of noise but with negative activation energy for both cases (exothermic and endothermic).

Keywords: CSTR, Exothermic, Endothermic, Random noise, Systematic random noise and Quasi random noise.

Declaration

I, the undersigned, hereby declare that the work contained in this research project is my original work, and that any work done by others or by myself previously has been acknowledged and referenced accordingly.

Jean Pierre MUHIRWA, 12th July 2015

Contents

List of Figures

Acronyms and Abbreviations

Table 1: Table of Acronyms and Abbreviations

Acronyms / Abbreviations	Explanations
CSTR	Continuously Stirred Tank Reactor
CSTRs	Continuously Stirred Tank Reactors
ODEs	Ordinary Differential Equations
SDEs	Stochastic Differential Equations
EKF	Extended Kalman Filter
MLE	Maximum Likelihood Estimation
MCMC	Markov Chain Monte Carlo
AMLE	Approximate Maximum Likelihood Estimation
AEM	Approximate Expectation Maximization
CSTM	Continuously Stochastic Time Modelling method
RE	Random Errors
SE	Systematic Errors
MPE	Mean of Parameter Errors
σ	Standard Deviation
μ	Mean
Exother / exother	Exothermic
Endother / endother	Endothermic
Temp / temp	Temperature
Concentr / concentr	Concentration
Resid / resid	Residuals
Cool / cool	Cooling
HOSM	High-Order Sliding Mode
SOM	Sliding-Order Mode

1. Introduction

In this chapter, we consider the background of our research study, state research motivation and objectives. We also give some preliminary definitions useful to our research and describe the overall outline of the research study.

1.1 Background of the Problem

Naturally, many systems have input and output flows and function over long time periods. We say that bioprocesses are continuous if active micro-organisms are available continuously. Man-made bioprocesses in the past were for useful products, however, these bioprocesses were rarely continuous since contamination is suspected when there is no control of the process against foreign organisms that may enter the system (RPI, Accessed 2015).

In 1857, Louis Pasteur discovered that micro-organisms were the cause of diseases and deterioration. During this period of time, the process of keeping food in a bioprocess had not been invented yet. A long time ago, waste treatment was continuous and an issue. However, they performed waste treatment by dumping it on land or throwing it into rivers' channels. The waste kept continuously coming, until the idea of a continuous process was discovered. This dates back to the 19th century where the continuous process was first invented by Novick (RPI, Accessed 2015). This reactor was used for converting waste beers and wines to vinegar. In this reactor, the bacterial populations of acetic acid were put onto the wood shavings. Drops of beer or wine were then put at the top of the reactor and allowed to flow through the shavings. Vinegar was collected through the outlet on the bottom of the reactor (RPI, Accessed 2015). To further develop the idea, a continuous stirred tank reactor (CSTR) was developed in the 1950's by Novick and Szilard (RPI, Accessed 2015) to study the behaviour of microbes. They realized that the continuous stirred tank reactor could be used to regularize the growth of microbes at certain values (steady state values). The discovery of the CSTR was very important in science since it changed traditional thinking that the growth of microbes become stable when they reach the maximum rate. Therefore, a well-mixed continuous reactor served as an instrument that helped to study and understand the behaviour of microbes, the cycle of cell, metabolic regulation, as well as microbial product formation (RPI, Accessed 2015).

Currently, the continuous stirred tank reactor is a process used in chemical engineering to produce products from the given input of substances. For example, the treatment of waste by producing organic fertilizers, electricity from biogas, production of chemical products (alcohols), polymerization etc. So, the chemical reactors are the most necessary and important units that chemical engineers have to take into consideration. Before estimating parameters, fitting and analysing continuously stirred tank reactor models, we have to understand how this process works and why it is important in chemical engineering reactions. To ensure the operation of the CSTRs work successfully, it is better to understand their dynamic characteristics as non-linear systems. A good understanding will automatically enable effective control of the system design. To describe the dynamic behaviour of the CSTR with **exothermic** or **endothermic** reactions, we have to take care of the **mass** component balance and **energy** component balance (Willis, 2000). Inside the CSTR, a reaction will produce new components (products) while on the other hand, reduces the concentration of the reactants. This process may cause exothermic reactions (which release heat energy) or endothermic reactions (which acquire heat energy) (Willis, 2000).

In chemical engineering reaction models, engineering modellers may encounter two types of problems

in parameter estimation. The first one appears when sophisticated mechanistic models are built and have a big number of unknown parameters to be estimated from the limited source of data. In this case, we might say that the structure of the model is complicated enough and it could qualify the behaviour of the process accurately, if and only if its accurate parameter values were provided (Karimi, 2013). The second problem that the simplified dynamic chemical models of the process may encounter is that the model structure may not be perfect for the unmeasured external disturbances and seems to be unreliable for future prediction, since this can influence the behaviour of the process. In this case, the modellers should have a considerable amount of data which facilitates parameter estimation. However, the mismatches of the model and random disruption (stochastic disturbance) must be taken into consideration (Karimi, 2013).

The complex ordinary differential equations (ODEs) that have non-linear parameters in the model are classified under the first type of model problems. In the second type of model problems, we classify differential equations for which, the stochastic terms (random terms) are added on the right hand-side of the ODEs to take into account disturbances and mismatch of the model. This leads to the stochastic differential equations (SDEs). The process of introducing random terms on ODEs is helpful for the improvement of parameter estimation and reliable model prediction. Therefore, knowing the strength of the model mismatch and disturbance may help in the implementation and the control of a dynamical process (Karimi, 2013).

To eradicate the two stated problems, several statistical methods have been developed. The most famous one is used in non-linear SDEs parameter estimation and is called the Extended Kalman Filter (EKF) (Kristensen and Madsen, 2003; Mbalawata et al., 2014). However, the performance of this method may be poor due to increase in bias and lack of convergence. This allows maximum likelihood estimation (MLE) to be a more preferred method to estimate the parameters, due to its convergence, consistency and efficiency in parameter estimation (Gandhi, 2009). The MLE method on the other hand has known difficulties due to conditional density functions in maximum likelihood algorithms with high-dimensional integrals that are not flexible to analytical simplifications (Gandhi, 2009). Moreover, many authors have proposed to use the Markov Chain Monte Carlo (MCMC) method; since it handles and approximates high-dimensional integrals (Mbalawata et al., 2014). However, the challenge of parameter estimation in stochastic differential equations still remains a big problem as the number of states (variables) and parameters increase in the process (Karimi, 2013). Therefore, none of the discussed methods above is optimal in solving the problem; due to the high cost (slow algorithm process to estimate the parameters), lack of convergence and computational complexity (Gandhi, 2009). In response to the weaknesses of the above methods, Vaziri and his colleagues in (Varziri et al., 2008) developed the Approximate Maximum Likelihood Estimation (AMLE). Other methods that can provide better estimate of parameters than the AMLE are the Approximate Expectation Maximization (AEM) and the Continuously Stochastic Time Modelling method (CSTM)(Karimi, 2013).

Another big challenge in parameters optimization is that sometimes there is unavailable information about the experiments, for instance, the real data of the system which can help to measure the robustness of the model. For our case (continuous stirred tank reactor), the true parameter values are not known; the only option is to guess the initial parameters. This parametric uncertainty has some important consequences. First, we expect to lose the potentiality of information about the system. So, experiments need to be robust with respect to the information content (Asprey and Macchietto, 2000). In (Korkel et al., 2004), it is suggested how to formulate the robust experiments, like design formulation as a max-min optimization loop explicitly with a linear approximation. The idea of expected value optimization for optimal experiment design objectives is introduced in (Bayard et al., 2013) and applied to a dynamic system for Gaussian distribution of the parameters in (Asprey and Macchietto, 2002). Nowadays, the

continuous stirred tank reactors are very useful in chemical engineering as tools that help to produce chemical products. Hence, to study their behaviour is very useful as it helps to design control against external disturbances. The motivation of our work is to see how uncertainties (errors) influence the model fitting and estimate the parameters of the CSTR. We will mainly focus on the simulations and the parameter estimation of the continuous stirred tank reactor by using different types and levels of noise, to track the influence of errors (uncertainties) in the model fitting, and the parameter estimation. Two parameters, the reaction rate k and the activation energy E were selected to be estimated in this project, in accordance with their sensitivities in the process.

1.2 Research Objectives

In every model fitting there are uncertainties in the parameter estimation that may have an impact on the model for future prediction. Therefore, it is necessary to test and analyse the strength of the model through parameter estimation. The main objective of this project is to study how different types and levels of noise in measurements influence the model fitting, parameter estimation and simulations of the continuously stirred tank reactor.

Specific objectives are:

- writing down model equations for the CSTR with the cooling jacket, heating jacket and compound inflow and outflow, both for the case of **exothermic** and **endothermic** reactions.
- implementing the numerical solutions of the system with fixed parameter values.
- generating the synthetic data by adding different types and levels of noise (random, quasi random and systematic random) to some of the component values obtained from the numerical solutions.
- analysing the influence and performance in model fitting and estimated parameters from different synthetic data compared to the true solutions (observations).

1.3 Preliminaries

In science, all taken measurements have errors (uncertainties) that are associated with them. These may come from the imprecision of measuring equipment or environmental disturbances in measurements. The errors are not "mistakes" or "blunders" as mentioned by (Karkalousos and Evangelopoulos, 2009). The three types of errors to be investigated in this work, are defined as follows:

1.3.1 Definition (Random errors): Random errors are called normal errors, Gaussian distribution errors or indeterminate errors. These errors are the kind of errors which appear in measurements randomly, and often cause the measurements to be larger or smaller than what it really is. The main characteristic of these errors is that, they deviate from the fitted model randomly (no patterns). Mathematically, random errors are defined as result of measurements minus the mean value that would result from several measurements performed at the same conditions on the same object (material). So, $RE = x_i - \bar{x}$ (Karkalousos and Evangelopoulos, 2009).

1.3.2 Definition (Systematic random errors): Systematic random errors are called bias errors or determinate errors. These errors always cause the measurements to be different from the real values of the measurements (always greater or smaller than true values of the measurements). These type of errors

emerge from the imprecision of the measuring instruments (poorly calibrated instruments) and they can be measured, corrected and adjusted. The main feature of these errors is that, they deviate from the fitted model by developing systematic patterns. Mathematically, they are defined as the average of several measurements of the same material performed at the same conditions minus the mean value of the true measurements of the object (material). So, $SE = \bar{x} - \mu$ (Karkalousos and Evangelopoulos, 2009).

1.3.3 Definition (Quasi random errors): Quasi random errors are defined as a sequence of n-tuples that fill n-dimensional space more uniformly than uncorrelated random points. They are also called low-discrepancy sequence. Sobol sequence is an example of the quasi random sequence that is more evenly distributed. There is a big difference between ordinary random noise and quasi random noise even though both produce random distributed noise. Random noise generators produce outputs so that each point has the same probability of occupying any space in a grid. This is not the case for the quasi random noise, since the outputs are limited by the low-discrepancy, and forces the points to be generated in a highly correlated procedure. So, the points are generated in a such away that the next point to be generated will know exactly where all previous generated points are located (Sahu, 2011).

1.4 Outline of the Project

In Chapter 1, we introduce the background of the problem, state our research objectives and give some useful definitions. Relevant research and past literature are reviewed in Chapter 2. In Chapter 3, we derive the model equations for both exothermic and endothermic CSTRs. Numerical simulations, analysis and discussion of the results are covered in Chapter 4. Our project ends with conclusion and recommendations in Chapter 5.

2. Literature Review

A lot of research has been done on parameter estimation and control of CSTRs. Some of the latest and recent research findings are mentioned in this project. In (Telen et al., 2014), sigma point method is used to robustify optimal experiment design (OED) for non-linear dynamic (bio)chemical systems. The sigma point method was used here because it has a robustifying effect and provides the efficient computation of the constraints variance-covariance matrix (fisher information matrix). They also investigated two kind of reactors: a well-mixed fed-batch reactor and the Williams-Otto reactor. For each case, two parameters were taken into consideration and estimated. The maximum specific growth rate μ_{max} and half-saturation constant K_s were estimated for the well-mixed fed-batch reactor. Also, as for the well-mixed fed-batch reactor, the kinetic coefficient of the reaction k_1 and the heat transfer l_1 were estimated from the Williams-Otto reactor, using the same method. After discretizing the differential equations for a well-mixed fed-batch reactor and using CasADi software, the numerical results showed that the largest difference with the nominal profile originates from sigma points π_1 and π_3; which influences μ_{max}. In investigating the influence of estimated parameters, the EE-design was proved to be more robust than the E-design. The authors here also showed the influence of a single parameter on the parameter estimation accuracy, expressed as the mean relative parameter error (MPE) measured in percentage. One parameter was fixed and other was varied up to 50%. Their results revealed that μ_{max} influenced MPE more than K_s. Therefore, if μ_{max} is fixed and is accurate, the value of K_s cannot easily influence the parameters accuracy for both designs. For the Williams-Otto reactor, three designs were considered, D-design, expected D-design (ED-design), and robustified expected D-design (robust ED-design). Through the discretization and sampling technique, they represented their numerical results graphically by the variation of k_1 versus l_1 as estimated parameters.

Karimi in (Karimi, 2013), investigated the effectiveness of three methods: the Approximate Expectation Maximization (AEM), the Approximate Maximum Likelihood Estimate (AMLE) and the Continuously Time Stochastic Modelling (CTSM) in approximating the parameters and disturbance intensities of the CSTR. He also estimated three parameters: Chemical reaction rate k, Activation energy E and heat transfer coefficient UA that depends on cooling rate and heat capacity. He further estimated the disturbance intensities for concentration and temperature using all the methods. From his simulations, the concentration of the substance and temperature were measured 100 times by randomly guessing initial parameters. Simulation results (done using the Matlab ode45 solver) showed that AEM is a better parameter estimator compared to CTSM and AMLE. He also, found that AMLE provided more bias in disturbance intensities estimates than the other two methods followed by CTSM. Therefore, he showed that AEM is a good estimator method for the CSTR with random disturbances; as it provides less variability in parameters and disturbance intensities estimates compared to AMLE and CTSM.

In (Osorio et al., 2011), the states and inputs in a continuous stirred tank reactor CSTR are investigated by comparing the accuracy of two observers: the high-order sliding mode observer (HOSM) and the first-order sliding mode observer (SOM). The considered observers here refers to the difference between the estimated values and the measured variables (true solutions) for each of the mode stated. The main aim of their work was to reduce the errors in the parameter estimation using HOSM. Results of their simulations and estimation of the parameters showed that the high-order sliding mode provide small errors for inputs concentration and temperature in the CSTR within minimum time compared to that of the SOM designer. The difference in results was due to the strength of the HOSM in minimizing the errors in parameter estimation.

In (Voros et al., 2008), the Extended Kalman Filter method was used to estimate the parameters for

an interacting tanks-in-series process, and to investigate the temperature of reaction mixture and the frequency for CSTRs. The Extended Kalman Filter method was used for the purpose of linearisation of CSTR models around the Kalman Filter estimate. The estimation of the parameters and states were observed by adding noise to the model. Simulations and parameter estimation results showed that the Extended Kalman Filter algorithm gives small errors from the true solutions. Also, the estimated parameters converge with the minimum time for different proposed initial values.

The behaviour of the CSTR was studied in (Vojtesek and Dostal, 2008) by analysing the dynamic and steady state behaviours of the system formulated by four differential equations of certain reactants. The standard Runge-Kutta's method (similar to ode45 solver in matlab software) was used for the numerical simulations. For the case of state of the system, concentrations of some substances reached their steady-state in a certain range of heat removal coefficients, as well as in a certain range of the reactive flow rate. They concluded that the heat removal and the flow rate range play an important role in the stability of the system. From the steady state, they obtained steady state values that were used as inputs to determine the dynamic behaviour of the system. In dynamic analysis, it was noted that a single change of input quantity of the heat removal and the reactive flow rate into the CSTR changes the steady state. As a result, both outputs were given by the difference between the variables and their steady state values. Those values were obtained by changing the heat removal and the reactive flow rate which were showed to have non-minimum phase behaviour as they change sign of static product. Hence, the change of the input values implies the decrease of maximum value of the variables.

Useful analysis of linear and non-linear system models such as CSTR models are greatly discussed in (Willis, 2000). Also, some basic concepts of chemical reaction models for the CSTR are derived and some simulations of the same reactor models are performed. Linearisation of components of the CSTR equations is considered using the Taylor series to obtain the approximate model of the CSTR. Moreover, the steady state of the system is investigated by taking one example of a reaction in the CSTR and the values of steady state for the concentration and temperature were calculated from the formulated model of the reaction.

Based on the above review, we aim to simulate and track how different types and levels of noise influence the model fitting and parameter estimation of continuously stirred tank reactors for the two cases of reactions, (exothermic and endothermic) using Minimization Assimilation method (least square method).

3. Model Equations

Every model has several assumptions to simplify the task or to make at least the outcomes of the model understandable. In this work, the models of the exothermic and endothermic continuously stirred tank reactors (CSTRs) have been constructed and analysed by considering the following assumptions (Willis, 2000):

- the volumes of the tank reactor, the cooling jacket and the heating jacket are constant.
- the area of heat transfer between the cooling or heating jacket and the tank reactor is constant.
- the dynamic temperature of the coolant or the heating substance is faster than the dynamic temperature of the substance inside the CSTR.
- specific heat capacities of the CSTR, cooling jacket and heating jacket are constants.
- the densities of substance inflow or outflow are constants.
- volumetric flows in and out of the tank reactor are the same.
- the rate of concentration in and out of the tank are the same.

Formulation of model equations of the CSTR is divided into two parts; exothermic with the cooling jacket and endothermic with the heating jacket.

3.1 Exothermic CSTR with the Cooling Jacket

Before talking about the continuously stirred tank reactor with the cooling jacket (cooling batch) which is the exothermic, we first consider the CSTR with no reaction inside the tank. To formalise this system we use **mass conservation law**, where the change of mass inside the tank is equal to the mass coming in minus the mass going out. Mathematically, we express this as:

$$\frac{\mathrm{d}m}{\mathrm{d}t} = C_{\text{in}}F - C_{\text{out}}F = (C_{\text{in}} - C_{\text{out}})\,F. \tag{3.1.1}$$

where C_{in} is the concentration of the substance coming into the tank, F is the volumetric flow of the substance and C_{out} is the concentration of the substance going out from the tank. If we divide on both sides of equation (3.1.1) by V, we obtain the change of concentration; that is given by:

$$\frac{1}{V}\frac{\mathrm{d}m}{\mathrm{d}t} = \frac{\mathrm{d}C(t)}{\mathrm{d}t} = (C_{\text{in}} - C_{\text{out}})\,\frac{F}{V}. \tag{3.1.2}$$

The ordinary differential equation shown in the equation (3.1.2) is the equation that governs the change of concentration inside a continuously stirred tank reactor with no reaction.

By adding a single input reactant (substance) with concentration $C(t)$ into the tank at time t, and by applying the law of conservation of mass, we obtain

[Change of mass in the tank] = [mass flows in] - [mass flows out].

During the reaction process inside the tank, there is also mass flows caused by reaction. Hence, the change of mass in the system is given by,

[Change of mass in the tank] = [mass flows in] - [mass flows out] + [mass flows due to reaction]. we know from kinetic reactions that, $\frac{\mathrm{d}C(t)}{\mathrm{d}t} = -kC(t)$, where k is the reaction rate. This implies that, the change in mass flow due to the reaction is given by,

$$\frac{\mathrm{d}m}{\mathrm{d}t} = V\frac{\mathrm{d}C(t)}{\mathrm{d}t} = -kVC(t).$$

By using mass conservation law, the mass in the system with single input reaction can be expressed mathematically as:

$$\frac{\mathrm{d}m}{\mathrm{d}t} = (C_{\text{in}} - C_{\text{out}})\,F - kVC(t). \tag{3.1.3}$$

Diving equation (3.1.3) by the volume V, we end up with,

$$\frac{1}{V}\frac{\mathrm{d}m}{\mathrm{d}t} = \frac{\mathrm{d}C(t)}{\mathrm{d}t} = (C_{\text{in}} - C_{\text{out}})\,\frac{F}{V} - kC(t). \tag{3.1.4}$$

The equation (3.1.4) is the simplest ordinary differential equation for the change of concentration of the reactants inside the CSTR.

Let us now complicate the model, by assuming that the reaction is exothermic (the reaction releases the heat energy). The procedure remains the same, we only need to introduce the governing equation for the change of temperature based on energy conservation from thermodynamic law. i.e., the change of energy E per unit of time. By using thermodynamic law, the temperature of the mass changes with rate $\frac{\mathrm{d}T}{\mathrm{d}t}$, and this is given by,

$$\frac{\mathrm{d}E}{\mathrm{d}t} = mC_p\frac{\mathrm{d}T(t)}{\mathrm{d}t}, \tag{3.1.5}$$

where C_p is the heat capacity of the tank measured in $[\frac{J}{kg^oK}]$. By the law of conservation of energy, the change of energy of the system is due to the change of the energy flows in and out, together with the energy flows caused by the reaction. So, the change of energy can be written as:

$$\frac{\mathrm{d}E}{\mathrm{d}t} = \frac{\mathrm{d}E_{\text{flows}}}{\mathrm{d}t} + \frac{\mathrm{d}E_{\text{reactions}}}{\mathrm{d}t}. \tag{3.1.6}$$

or

$$\frac{\mathrm{d}E}{\mathrm{d}t} = \frac{\mathrm{d}E_{\text{flows in}}}{\mathrm{d}t} - \frac{\mathrm{d}E_{\text{flows out}}}{\mathrm{d}t} + \frac{\mathrm{d}E_{\text{reactions}}}{\mathrm{d}t}.$$

But,

$$\frac{\mathrm{d}E_{\text{flows}}}{\mathrm{d}t} = C_p\frac{\mathrm{d}m}{\mathrm{d}t}\left(T_{\text{in}} - T(t)\right). \tag{3.1.7}$$

where $T(t) = T_{\text{out}}$, $\frac{\mathrm{d}m}{\mathrm{d}t}$ is the mass flow rate $[\frac{kg}{s}]$, T_{in} is the temperature of the substance flowing in and $T(t)$ is the temperature at time t in the tank, which is equal to the temperature of the products flowing out from the tank.

The energy change rate due to the reaction itself is given by,

$$\frac{\mathrm{d}E_{\text{reactions}}}{\mathrm{d}t} = (\Delta H)r(T)V, \tag{3.1.8}$$

where ΔH is the reaction **enthalpy** $[\frac{J}{mole}]$, which is the energy released or required for 1 **mole** of the substance to be transformed and $r(T)$ is the concentration rate given in $[\frac{\text{mole}}{m^3 s}]$.

Putting equations (3.1.7) and (3.1.8) into equation (3.1.6) we obtain,

$$\frac{\mathrm{d}E}{\mathrm{d}t} = C_p \frac{\mathrm{d}m}{\mathrm{d}t} (T_{\text{in}} - T(t)) + V(\Delta H) r(T). \tag{3.1.9}$$

From equations (3.1.5) and (3.1.9) we have,

$$mC_p \frac{\mathrm{d}T(t)}{\mathrm{d}t} = C_p \frac{\mathrm{d}m}{\mathrm{d}t} (T_{\text{in}} - T(t)) + V(\Delta H) r(T).$$

Substituting $m = \rho V$ and $\frac{\mathrm{d}m}{\mathrm{d}t} = \rho F$, where F is the volumetric flow rate $[\frac{m^3}{s}]$ and ρ the density of the substance $[\frac{kg}{m^3}]$, the equation of the energy becomes,

$$\rho V C_p \frac{\mathrm{d}T(t)}{\mathrm{d}t} = \rho F C_p (T_{\text{in}} - T(t)) + V(\Delta H) r(T).$$

Dividing both sides by $\rho C_p V$ yields,

$$\frac{\mathrm{d}T(t)}{\mathrm{d}t} = \frac{F}{V} (T_{\text{in}} - T(t)) + \frac{(\Delta H) r(T)}{\rho C_p}. \tag{3.1.10}$$

The equation (3.1.10) is the change of energy equation of the CSTR with reaction at time t.

Grouping together equations (3.1.4) and (3.1.10) we have,

$$\begin{aligned} \frac{\mathrm{d}C(t)}{\mathrm{d}t} &= (C_{\text{in}} - C_{\text{out}}) \frac{F}{V} - kC(t), \\ \frac{\mathrm{d}T(t)}{\mathrm{d}t} &= \frac{F}{V} (T_{\text{in}} - T(t)) + \frac{(\Delta H) r(T)}{\rho C_p}, \end{aligned} \tag{3.1.11}$$

where k is the reaction rate that depends on the temperature according to Arrhenius law. So, $k = k_{\text{mean}} e^{-\frac{E}{R(\Delta T)}}$ and $r(T) = k \times reactants = kC(t)$ is the concentration rate. E is the Activation energy, k_{mean} is the Arrhenius pre-exponential factor and R is the gas law constant.

For the exothermic reaction we need to have a cooling jacket that helps to cool down the temperature (heat energy). Therefore, we build the model equations by considering the following diagram (Kauranne, Accessed in June, 2015).

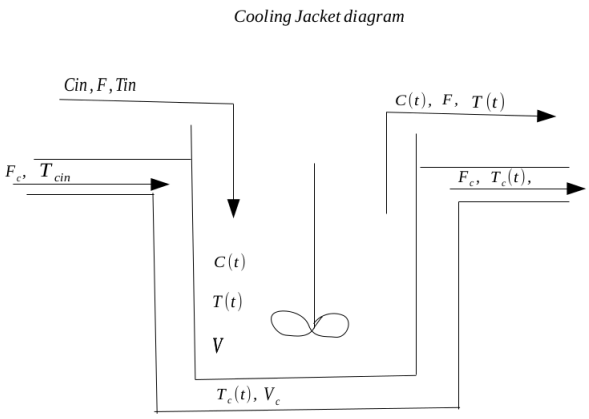

Figure 3.1: This diagram is adopted from (Kauranne, Accessed in June, 2015).

$C(t), T(t)$ and V, represent the concentration, temperature and volume of the tank respectively at time t. $C_{\text{in}}, T_{\text{in}}$ and F represent the concentration, temperature and the rate of change of the feeds in the tank respectively. $T_c(t)$ and V_c represent the temperature and volume of the cooling jacket respectively. T_{cin} and F_c represent the temperature and feed rate of the cooling substance (coolant) respectively.

The equation (3.1.11) is without a cooling jacket but now we want to introduce a cooling jacket into the system. By doing so, the energy in the CSTR decreases by

$$\frac{UA}{\rho V C_p}\left(T(t) - T_c(t)\right).$$

So, equation (3.1.11) becomes,

$$\frac{\mathrm{d}T(t)}{\mathrm{d}t} = \frac{F}{V}\left(T_{\text{in}} - T(t)\right) + \frac{(\Delta H) r(T)}{\rho C_p} - \frac{UA}{\rho V C_p}\left(T(t) - T_c(t)\right),$$

where U is the heat transfer coefficient and A is the heat transfer surface area.

In a similar way, energy balance at the cooling jacket is determined as follows:

$$\frac{\mathrm{d}T_c(t)}{\mathrm{d}t} = \frac{F_c}{V_c}\left(T_{\text{cin}} - T_c(t)\right) + \frac{UA}{\rho_c V_c C_{pc}}\left(T(t) - T_c(t)\right),$$

where ρ_c is the density of the coolant and C_{pc} is the heat capacity of the cooling jacket. Again, using mass conservation law, from equation (3.1.4) we get

$$\frac{\mathrm{d}C(t)}{\mathrm{d}t} = \frac{F}{V}\left(C_{\text{in}} - C(t)\right) - r(T), \tag{3.1.12}$$

where $r(T)$ is the temperature dependent concentration rate given by, $r(T) = kC(t)$ and k is given by the Arrhenius equation. Therefore, the governing equations of the **exothermic** CSTR with the cooling jacket are:

$$\frac{\mathrm{d}T(t)}{\mathrm{d}t} = \frac{F}{V}\left(T_{\text{in}} - T(t)\right) + \frac{(\Delta H) r(T)}{\rho C_p} - \frac{UA}{\rho V C_p}\left(T(t) - T_c(t)\right), \tag{3.1.13}$$

$$\frac{\mathrm{d}T_c(t)}{\mathrm{d}t} = \frac{F_c}{V_c}\left(T_{\text{cin}} - T_c(t)\right) + \frac{UA}{\rho_c V_c C_{pc}}\left(T(t) - T_c(t)\right), \tag{3.1.14}$$

$$\frac{\mathrm{d}C(t)}{\mathrm{d}t} = \frac{F}{V}\left(C_{\text{in}} - C(t)\right) - r(T). \tag{3.1.15}$$

Since the system is **exothermic**, it releases heat energy. Thus, the enthalpy has to be negative and the equation (3.1.13) becomes,

$$\frac{\mathrm{d}T(t)}{\mathrm{d}t} = \frac{F}{V}\left(T_{\text{in}} - T(t)\right) - \frac{(\Delta H) r(T)}{\rho C_p} - \frac{UA}{\rho V C_p}\left(T(t) - T_c(t)\right).$$

Therefore, the equations governing the **exothermic** CSTR are:

$$\begin{cases} \frac{\mathrm{d}T(t)}{\mathrm{d}t} &= \frac{F}{V}\left(T_{\text{in}} - T(t)\right) - \frac{(\Delta H) r(T)}{\rho C_p} - \frac{UA}{\rho V C_p}\left(T(t) - T_c(t)\right), \\ \frac{\mathrm{d}T_c(t)}{\mathrm{d}t} &= \frac{F_c}{V_c}\left(T_{\text{cin}} - T_c(t)\right) + \frac{UA}{\rho_c V_c C_{pc}}\left(T(t) - T_c(t)\right), \\ \frac{\mathrm{d}C(t)}{\mathrm{d}t} &= \frac{F}{V}\left(C_{\text{in}} - C(t)\right) - r(T). \end{cases} \tag{3.1.16}$$

Putting $r(T) = kC(t) = k_{\text{mean}} e^{-\frac{E}{R(\Delta T)}} C(t)$ into the system of equations (3.1.16) we obtain,

$$\begin{cases} \frac{\mathrm{d}T(t)}{\mathrm{d}t} & = \frac{F}{V}\left(T_{\text{in}} - T(t)\right) - \frac{(\Delta H) k_{\text{mean}} e^{-\frac{E}{R(\Delta T)}} C(t)}{\rho C_p} - \frac{UA}{\rho V C_p}\left(T(t) - T_c(t)\right), \\ \frac{\mathrm{d}T_c(t)}{\mathrm{d}t} & = \frac{F_c}{V_c}\left(T_{c\text{in}} - T_c(t)\right) + \frac{UA}{\rho_c V_c C_{pc}}\left(T(t) - T_c(t)\right), \\ \frac{\mathrm{d}C(t)}{\mathrm{d}t} & = \frac{F}{V}\left(C_{\text{in}} - C(t)\right) - k_{\text{mean}} e^{-\frac{E}{R(\Delta T)}} C(t). \end{cases} \tag{3.1.17}$$

These are the equations that describe continuously stirred tank reactor with the cooling jacket.

3.2 Endothermic CSTR with the Heating Jacket

Below is the schematic diagram that depicts a CSTR with a heating jacket (endothermic case).

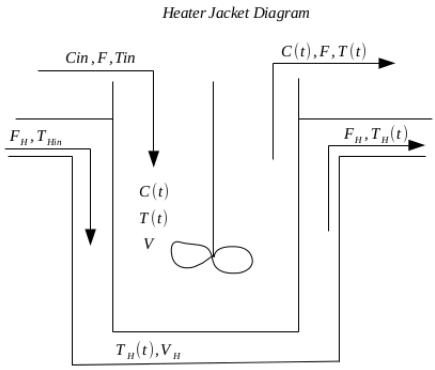

Figure 3.2: Graph describing the heating jacket and is constructed based on the CSTR with the cooling jacket (exothermic case).

The procedure of building the model equations is the same as for the exothermic CSTR, except that in this case the system absorbs heat energy for the reaction to take place. Therefore, **enthalpy** becomes positive and the energy due to the heating process (heat transfer term) becomes positive. So, the governing model equations are obtained by modifying the system of equations (3.1.16).

$$\begin{cases} \frac{\mathrm{d}T(t)}{\mathrm{d}t} & = \frac{F}{V}\left(T_{\text{in}} - T(t)\right) + \frac{(\Delta H) r(T)}{\rho C_p} + \frac{UA}{\rho V C_p}\left(T_H(t) - T(t)\right), \\ \frac{\mathrm{d}T_H(t)}{\mathrm{d}t} & = \frac{F_H}{V_H}\left(T_{H\text{in}} - T(t)\right) - \frac{UA}{\rho_H V_H C_{pH}}\left(T_H(t) - T(t)\right), \\ \frac{\mathrm{d}C(t)}{\mathrm{d}t} & = \frac{F}{V}\left(C_{\text{in}} - C(t)\right) - r(T). \end{cases} \tag{3.2.1}$$

By substituting the value of $r(T) = kC(t) = k_{\text{mean}} e^{-\frac{E}{R(\Delta T)}} C(t)$ into the system of equations (3.2.1) we end up with,

$$\begin{cases} \frac{\mathrm{d}T(t)}{\mathrm{d}t} & = \frac{F}{V}\left(T_{\text{in}} - T(t)\right) + \frac{(\Delta H) k_{\text{mean}} e^{-\frac{E}{R(\Delta T)}} C(t)}{\rho C_p} + \frac{UA}{\rho V C_p}\left(T_H(t) - T(t)\right), \\ \frac{\mathrm{d}T_H(t)}{\mathrm{d}t} & = \frac{F_H}{V_H}\left(T_{H\text{in}} - T(t)\right) - \frac{UA}{\rho_H V_H C_{pH}}\left(T_H(t) - T(t)\right), \\ \frac{\mathrm{d}C(t)}{\mathrm{d}t} & = \frac{F}{V}\left(C_{\text{in}} - C(t)\right) - k_{\text{mean}} e^{-\frac{E}{R(\Delta T)}} C(t). \end{cases} \tag{3.2.2}$$

which are governing CSTR equations with the heating jacket. Therefore, the task for endothermic CSTR becomes similar to the one of the exothermic CSTR with the cooling jacket.

4. Numerical Simulations and Results

This part of our work shows the results achieved by doing simulations and parameter estimation. Since we are dealing with two cases, the exothermic continuously stirred tank reactor and endothermic continuously stirred tank reactor, together with three types of noise, the results are categorized into three sections.

The first section shows the effect of random noise on parameter estimation and the model fitting for both cases of CSTRs. The second section contains the results on parameter estimation and model fitting of exothermic and endothermic CSTRs together with the quasi random noise. The third section covers the effect of systematic random noise on the two cases. The software employed in simulations and estimating parameters is scilab. The ode solver in scilab was used to solve the three ordinary differential equations formulated from the continuously stirred tank reactor (CSTR) for both cases of exothermic and endothermic reactions.

We have fixed the true parameters to be $k = 0.9$, $E = 0.5$ for the exothermic CSTR case and $k = 0.4$, $E = 0.5$ for the endothermic CSTR case. By introducing different types and levels of noise in the numerical solutions of concentration and temperature, we are able to generate synthetic data, taken as the measurements of the continuously stirred tank reactor with exothermic and endothermic reactions at time t. Therefore, this noisy data will help us to estimate the reaction rate $k = k_{\text{mean}} e^{\frac{-E}{R(\Delta T)}}$ that is dependent on temperature (Arrhenius Law) and the activation energy E using the Minimization Assimilation method (the least square method). Both parameters will contribute to the model fitting and help to track the influence of uncertainties to the parameter estimation and model mismatch.

We have run our simulations 5 times by guessing the initial values of parameters (initial guesses). These initial guesses were chosen based on the following criteria: by fixing higher values than the true parameters, higher values than the true parameters but closer, less values than the true parameters but closer, small values compared to the true parameters and the last guess become true parameters. The highest initial guess of values is $[1, 1]$ for all cases of the exothermic and endothermic CSTR. Higher but closer initial values are $[1, 0.6]$ and $[0.5, 0.6]$ for the exothermic and endothermic cases respectively. Less but closer initial guesses are $[0.8, 0.4]$ for exothermic case and $[0.3, 0.4]$ for endothermic case. A very less initial guess of values is $[0.1, 0.1]$ for all cases whereas the last guesses are $[0.9, 0.5]$ and $[0.4, 0.5]$ for the exothermic and endothermic CSTRs respectively. The first value in the brackets represents the initial guess for the reaction rate k whilst the second is the guess for the activation energy E. All the initial guesses always give the same estimated values of k and E depending on the type of CSTR, type of noise and level of noise.

The simulations were facilitated by the constants values and the parameters that are described in Table 4.1.

Table 4.1: Table of Variables and Constants

Variables and constants	Descriptions	Values	Units
$C(t)$	Concentration at time t	to be computed	$\frac{\text{mole}}{m^3}$
$T(t)$	Temperature of the reactor at time t	to be computed	^oK
R	Gas law constant	8.314	$\frac{Nm^3}{s}$
T_{mean}	Mean of temperature	298.15	^oK
k_{mean}	Pre-exponential Arrhenius factor	to be computed	No unit
k	Reaction rate	to be estimated	No unit
E	Activation energy	to be estimated	J
$r(T)$	Concentration rate	to be computed	$\frac{\text{mole}}{m^3 s}$
F	Volumetric flow rate in or out of tank	130×10^{-6}	$\frac{m^3}{s}$
V	Volume of reactor	110×10^{-6}	m^3
ΔH	Enthalpy for the endothermic and exothermic	10043×10^2 and -10043×10^2	$\frac{J}{\text{mole}}$
C_{in}	Concentration of substance flows into tank	316.8	$\frac{\text{mole}}{m^3}$
t	Time interval	$[0:20]$	s
ρ	Density of the substance in reactor	1000	$\frac{kg}{m^3}$
c_p	Heat capacity of reactor	4186	$\frac{J}{kg^oK}$
T_{in}	Temperature of the substance flows into tank	$25^0C = 298.35^0K$	^oK
U	Heat transfer coefficient	10000	No unit
A	Heat transfer area	0.015	m^2
$T_H(t)$	Temperature of the heating jacket at time t	to be computed	^oK
F_H	Volumetric flow rate of the heating substance	465×10^{-7}	$\frac{m^3}{s}$
V_H	Volume of the heating jacket	50×10^{-6}	m^3
ρ_H	Density of the heating substance	1000	$\frac{kg}{m^3}$
c_{pH}	Heat capacity of heating jacket	4186	$\frac{J}{kg^oK}$
$T_{H\text{in}}$	Temperature of the heating substance	288.15	^oK
$T_c(t)$	Temperature of cooling Jacket at time t	to be computed	^oK
ρ_c	Density of the cooling substance	1000	$\frac{kg}{m^3}$
c_{pc}	Heat capacity of the cooling Jacket	4186	$\frac{J}{kg^oK}$
F_c	Volumetric flow rate of the coolant	465×10^{-7}	$\frac{m^3}{s}$
V_c	Volume of the cooling Jacket	50×10^{-6}	m^3
$T_{c\text{in}}$	Temperature of the cooling substance	288.15	^oK

The values in Table 4.1 were taken from scilab scripts (programs). Especially, from cstr-cool-ode.sci and cstr-cool-ode1.sci (Kauranne, Accessed in June, 2015).

4.1 Random Noise

Random noise is introduced to the concentration and temperature solutions (numerical solutions) of the system to investigate the change of the parameters compared to the true parameters and true solutions compared to the simulated solutions. In this case, we have considered two levels of noise $\sigma = 2$ and

$\sigma = 10$ for both cases of the exothermic and endothermic CSTRs. We chose two levels of random noise, by taking the small variance to be 4 and the big variance to be 100 as they may not have the same effect.

4.1.1 Exothermic CSTR

Figure 4.1 represents the true solutions and noisy solutions of the exothermic CSTR. When $\sigma = 2$, we have the true solutions (numerical solutions) graph, the noisy solutions and the fitted graphs of CSTR with the exothermic reactions.

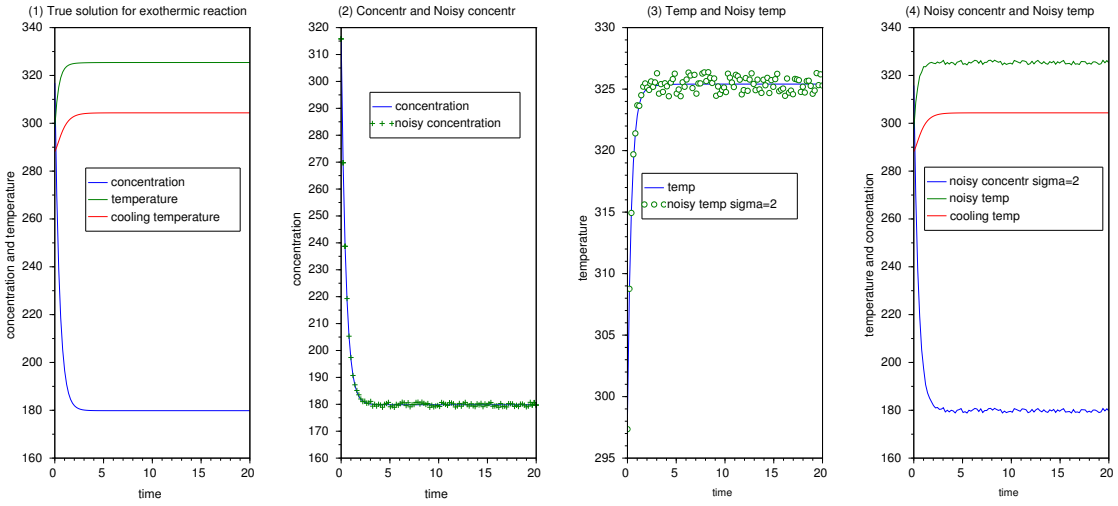

Figure 4.1: Graphs showing the numerical solutions of the exother CSTR model. Graph (1) shows the true solutions. Graphs (2),(3) and (4) show random noisy solutions. Parameters used are; $k = 0.9$ and $E = 0.4$. The parameter $\sigma = 2$ is used to generate the random noisy solutions.

From sub-plot (1) in Figure 4.1, we observe that the concentration of the reactants decrease from 316 and reaches its equilibrium state at 180 after 4 seconds. Also, from the same sub-plot, the coolant enters the system with a low temperature to cool down the temperature of the system. In the cooling process, the coolant temperature increases meanwhile the system temperature slow down until both temperatures become stable.

For $\sigma = 2$, the fitted curves and the residuals graphs are as shown in Figure 4.2.

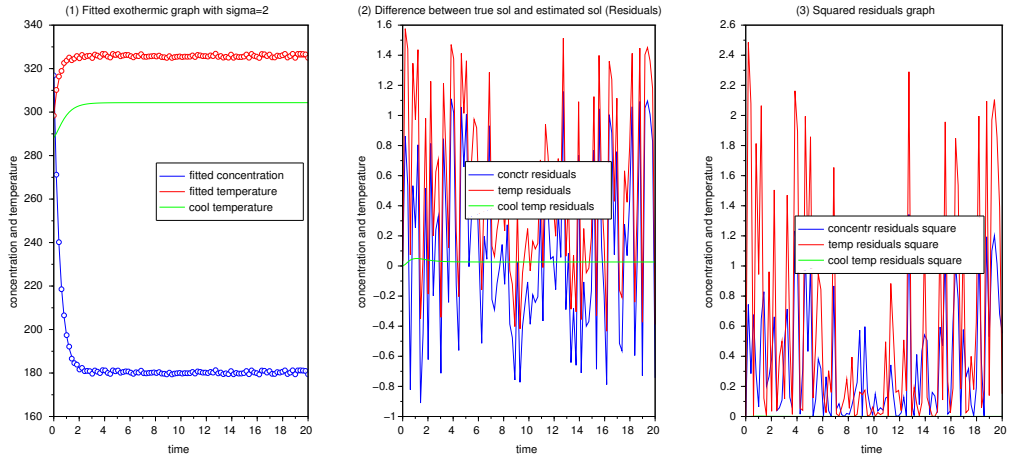

Figure 4.2: Graphs (1), (2) and (3) respectively show the model fitting, residuals and squared residuals of exothermic CSTR model. $\sigma = 2$ and the true parameters $k = 0.9$ and $E = 0.5$ are involved in numerical simulations. Estimated parameters are $k = 0.8853$ and $E = 377.2327$.

From Figure 4.2, the result shows that the estimated reaction rate approaches the true value with the difference of 0.0147 while the activation energy is too far from its true value. In sub-plot (2), more residuals of temperature are above zero in a scale of $[-0.4, 1.59]$, which indicates that more temperature observations are greater than the estimated temperature of the reactor. This is not the case for concentration residuals since almost 50% of the observations are greater than the estimated concentration while almost the other 50% are lower in the range $[-0.9, 1.1]$. The difference between the observations and the estimated values is not very significant since the scale of residuals is small. In sub-plot (3), the squared residuals are varying in the range $[0, 1.34]$ and $[0, 2.49]$ with the mean values of 0.34584 and 0.5917550 for the concentration and temperature respectively. We cannot observe the squared residuals of the cooling temperature on the squared residuals graph because they are around 0 with a very small mean value of 0.00082698. Hence, the results are quite good as the variation of residuals is at a low scale with small mean values. Therefore, the data is fitting the model well.

We now repeat the above simulations when $\sigma = 10$. The results are as shown in Figures 4.3 and 4.4.

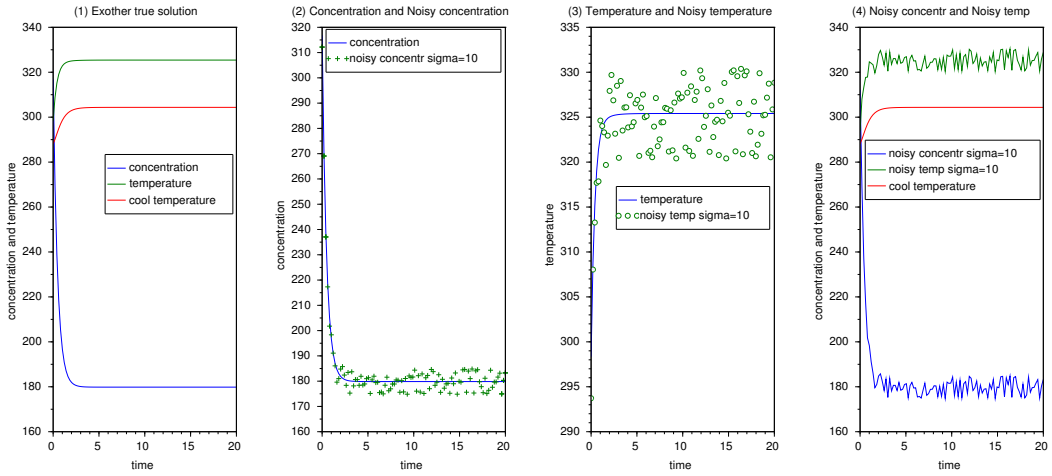

Figure 4.3: Graphs showing the numerical simulations of the exothermic CSTR model. Sub-plot (1) shows the true solutions. Sub-plots (2),(3) and (4) show random noisy solutions. True parameters used are $k = 0.9$ and $E = 0.5$. Noise level is given by $\sigma = 10$.

In Figure 4.3, we can see that data is spreading randomly along the true solution curves. Therefore, high randomness in the concentration and temperature of the reactor is observed compared to the randomness viewed in Figure 4.1.

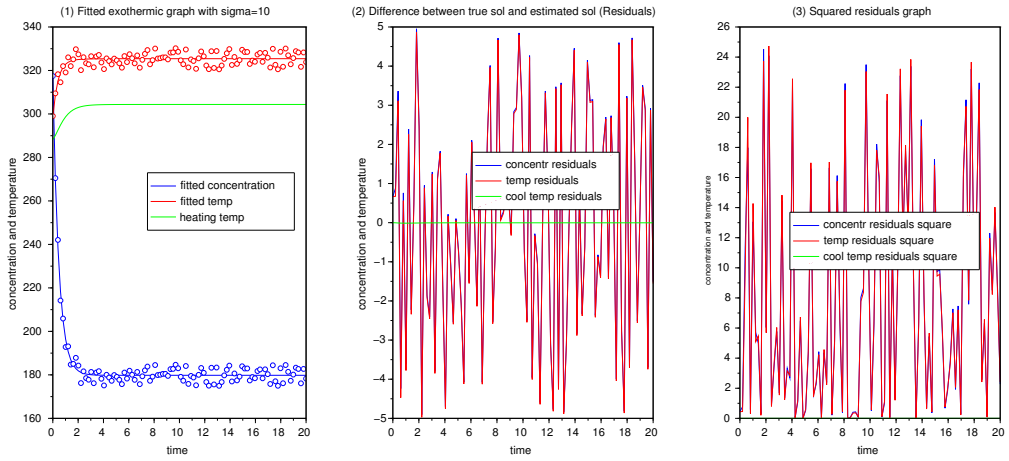

Figure 4.4: Graphs (1), (2) and (3) respectively show the model fitting, residuals and squared residuals of the exothermic CSTR model. $\sigma = 10$ and the true parameters are $k = 0.9$ and $E = 0.5$. Estimated parameters from Minimization Assimilation method are $k = 0.9044$ and $E = -129.39$.

In Figure 4.4, the estimated reaction rate is greater but converges to its true value with the difference of 0.0044 while the activation energy becomes negative and diverges from its true value. The negative value for the activation energy, physically indicates that the reaction cannot be stopped, unless the reactants are kept away from the tank. In sub-plot (2), the scale of concentration and the temperature residuals

becomes high and ranges between -5 and 5 . This implies that the significance of the difference between the observations and the estimated values of the temperature and concentration is considerable. In sub-plot (3), the squared residuals of the concentration vary in $[0, 24.53]$ with the mean value of 7.8652, and the squared residuals of the temperature range from 0 up to 24.74 with the mean value of 7.8723. The squared residuals of the cooling temperature vary near zero with the mean value of 0.000023. Hence, the variation and mean values of the squared residuals of the concentration and temperature increase. This is the reason why the data does not fit the model well.

4.1.2 Endothermic CSTR

This subsection is devoted to the endothermic continuously stirred tank reactor. The results are produced from random noise. Random noise is introduced in the numerical solutions of the concentration and temperature of the endothermic continuously stirred tank reactor (CSTR) model with the heating jacket. The same levels of standard deviation (low and high variances) means $\sigma = 2$ and $\sigma = 10$ are considered here. The graphs from Figure 4.5 to Figure 4.8 illustrate the simulations and the estimated parameters from the endothermic CSTR model with random noise $\sigma = 2$ and $\sigma = 10$.

Case 1: $\sigma = 2$

When $\sigma = 2$, the true solutions, the random noisy solutions and the fitted model with its estimated parameters for the endothermic CSTR are shown in Figures 4.5 and 4.6.

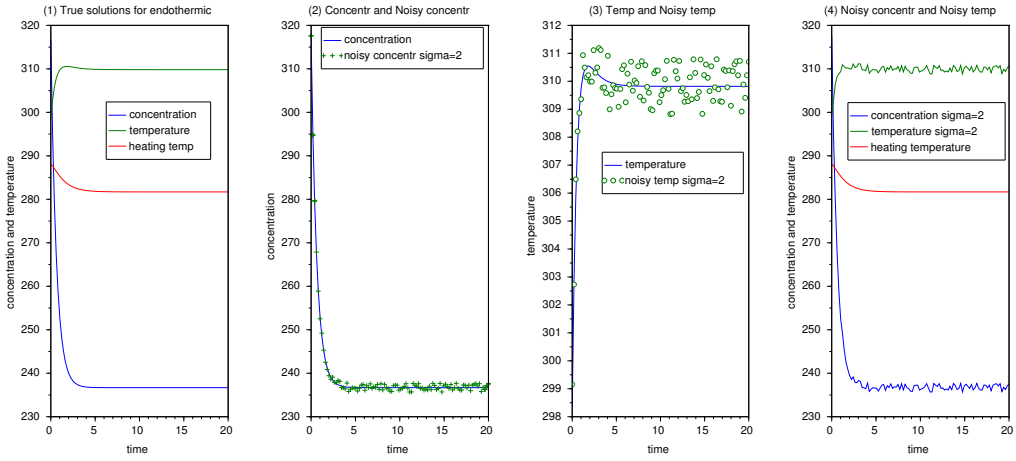

Figure 4.5: Graphs showing the numerical solutions of the endothermic CSTR model. Graph (1) shows the true solutions. Graphs (2),(3) and (4) depict random noisy solutions. Parameters used are; $k = 0.4$ and $E = 0.5$. The parameter $\sigma = 2$ is used to generate the random noisy solutions.

In Figure 4.5, sub-plot (1) shows that the concentration of the reactants decreases from 316 and reaches its equilibrium state at 248 after 5 seconds. Also, it indicates that the heating substance enters the system with a high temperature to catalyse the reaction. In the heating process, the temperature of the system increases while the heating temperature reduces, until both temperatures stabilize. In sub-plots (2) (3), and (4), the noisy solutions data are randomly spreading around both sides of the concentration and temperature true solution curves.

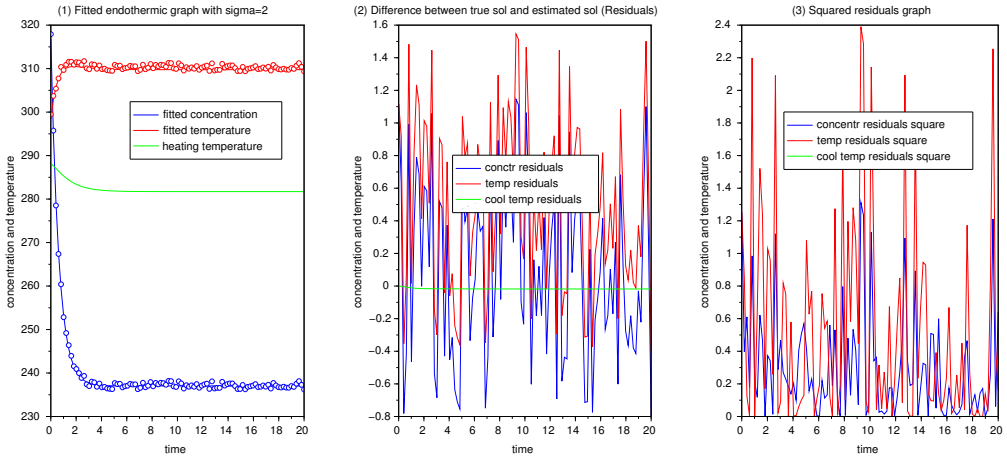

Figure 4.6: Graphs (1), (2) and (3) respectively represent the model fitting, residuals and squared residuals of the endothermic CSTR model. The level of noise is $\sigma = 2$ and the true parameters involved in numerical implementation are $k = 0.4$ and $E = 0.5$. Estimated parameters from Minimization Assimilation method become $k = 0.3948$ and $E = 485.69$.

The results obtained from Figure 4.6 also look good as the reaction rate is closer to its true value with only a difference of 0.0052, although the activation energy does not converge. It is however among the smallest values compared to the estimated activation energies obtained in this work. In sub-plot (2), the scale of concentration residuals is $[-0.8, 1.7]$ while the temperature residuals are skewed and almost a half of them are greater than zero on a scale of $[-0.4, 1.58]$. The difference between the observations and the estimated values of the concentration and the temperature is not high. The squared residuals of the concentration range between 0 and 1.31 with the mean value of 0.3028747 and the squared residuals of the temperature vary in the range $[0, 2.4]$ with the mean value of 0.5334537. The mean value of the squared residuals of the heating temperature is 0.00029228. Fortunately, good fitting can be seen in Figure 4.6, as most of the data points are in a margin of fitting the curves.

Case 2: $\sigma = 10$

When $\sigma = 10$, the true solutions, the random noisy solutions and the fitted model with its estimated parameters for endothermic CSTR are shown in Figures 4.7 and 4.8.

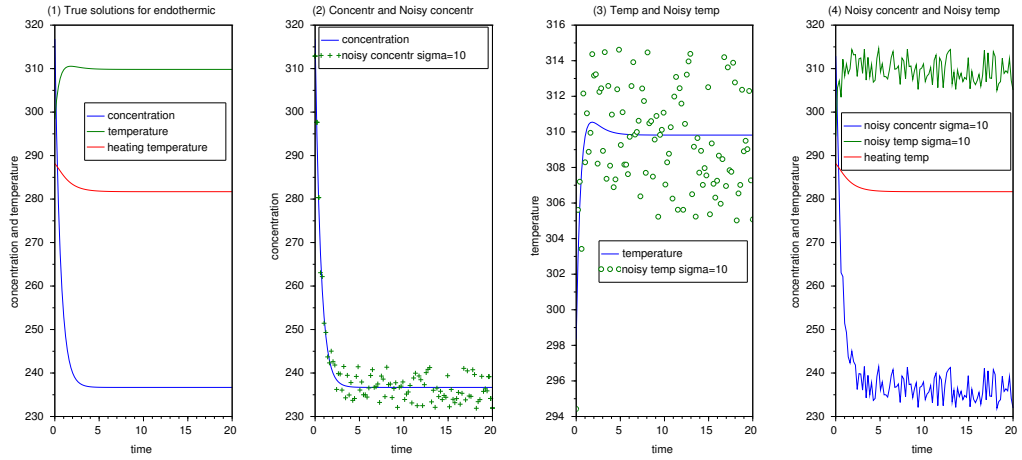

Figure 4.7: Graphs illustrating the numerical simulations of the endothermic CSTR model. Sub-plot (1) shows the true solutions. Sub-plots (2) and (3) show the noisy concentration and noisy temperature respectively while sub-plot (4) combines the true solutions and random noisy solutions. The experimental parameters are $k = 0.4$ and $E = 0.5$. The level of random noise is determined by $\sigma = 10$.

Figure 4.7 shows high scattering in data because of the increase of noise in the true solutions.

The fitting model and the residuals graphs of CSTR with the endothermic reaction when $\sigma = 10$ are as represented in Figure 4.8.

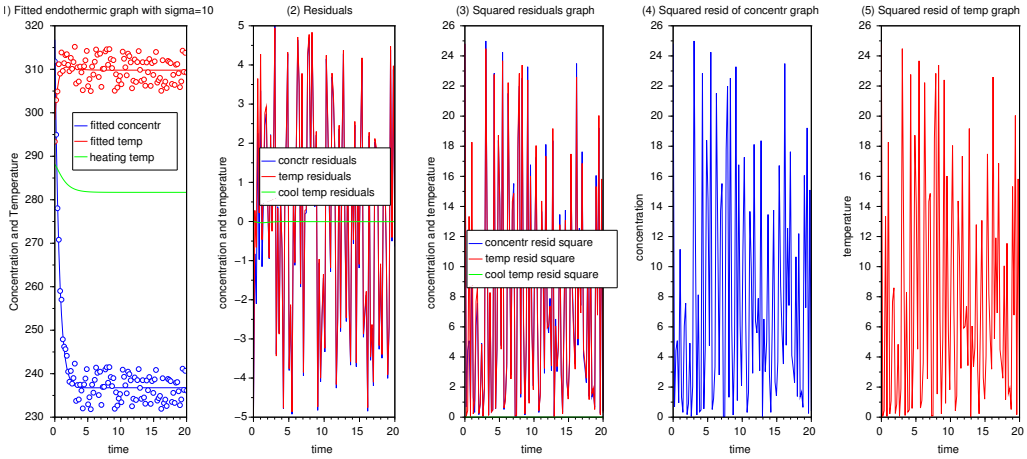

Figure 4.8: Graphs representing the endothermic CSTR model. Sub-plot (1) points out both fitting concentration and temperature curves. Sub-plot (2) shows the residuals while sub-plots (3), (4) and (5) show the squared residuals. The experimental parameters are $k = 0.4$ and $E = 0.5$ whilst estimated parameters are $k = 0.3782$ and $E = 3606.8$. The level of random noise is given by $\sigma = 10$.

The result shows that the variability in the reaction rate has increased slightly with the difference of 0.0218 and the activation energy remains large compared to the results obtained in Figure 4.6. The

range of residuals has also increased and becomes $[-5, 5]$ for both temperature and concentration. Almost half of the residuals are above zero while the other half are below zero. This implies that almost 50% of the observations are greater than the estimated values while the other 50% are less than the estimated temperature and concentration. The difference between observations and the estimated values is significant since more of the residuals are not around zero. The residuals of concentration squared vary in the range $[0, 25]$ with the mean value of 7.7814381 whereas the squared residuals of temperature vary between 0 and 24.8 with the mean value of 7.8997289, as can be seen in sub-plots (4) and (5) of Figure 4.8. The obtained mean value of the squared residuals of the heating temperature is 0.000086324, which is very small and negligible. Few data points among hundred fit the model while others are far away from the estimated model.

4.2 Quasi Random Noise

Quasi random noise is introduced in the obtained concentration and temperature numerical solutions for both continuously stirred tank reactors (based on exothermic and endothermic reactions). The purpose is the same as for the random noise. Therefore, in this section we will track the impact of quasi random noise to the parameter estimation and the model fitting of both CSTRs. Two levels of noise; $\sigma = 2$ and $\sigma = 10$ which are used in each section of this chapter, are again used here. The same R-code is used to produce quasi random noise that is, the Sobol sequence.

4.2.1 Exothermic CSTR

In this subsection, we have the true numerical solution curves, noisy numerical solution curves, the fitted curves, the estimated parameters and the residual graphs for the exothermic continuously stirred tank reactor (CSTR). Quasi random noise is introduced to the temperature and concentration solutions obtained from numerical implementation of the models using the true parameters $k = 0.9$ and $E = 0.5$. We were able to generate the quasi random noisy solutions taken as the measurements of the concentration and temperature of the system at time t. We used these measurements to simulate and estimate the parameters of the exothermic CSTR, in a process of investigating the effect of this type of noise to the system. The quasi random noisy data in this work is generated using R-code as previously said. One hundred data points are generated to match the dimension of the numerical solutions given by the odesolver in scilab. The same levels of noise $(\sigma = 2)$ and $(\sigma = 10)$ are considered here, so that, we may decide which type of noise or which level of noise has great impact on the parameter estimation and model fitting for both cases of exothermic and endothermic reactions.

We first investigate the effect of quasi random noise, produced using $\sigma = 2$. The results are as shown in Figures 4.9 and 4.10.

Figure 4.9 shows the true solutions and quasi random noisy solutions.

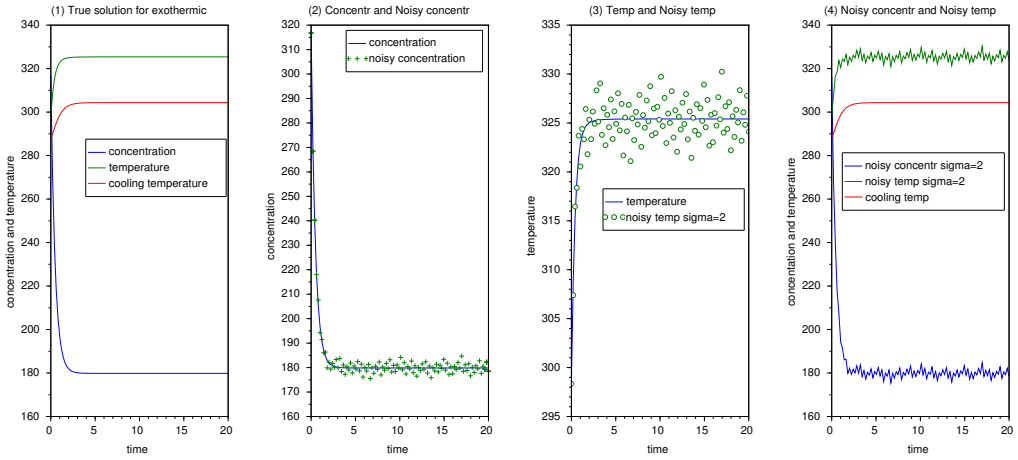

Figure 4.9: Graphs showing the numerical solutions and noisy solutions of the exothermic CSTR model. The considered noise is quasi with $\sigma = 2$. Sub-plot (1) shows the numerical true solutions, sub-plots (2) and (3) represent the concentration and temperature with quasi random noise respectively. Sub-plot (4) includes both numerical solutions and noisy solutions. The experimental parameters are $k = 0.9$ and $E = 0.5$.

From the definition of quasi random noise, we observe quasi random noisy data around the concentration and the temperature solutions of the exothermic CSTR, in sub-plots (2), (3)and (4) of Figure 4.9 from left to right. This type of noise has the feature of high correlation in the data since each point is located according to the locations of other points. So, the patterns of the oblique correlation are observed in sub-plots (2) and (3) of Figure 4.9.

The fitted curves and the residual graphs of the exothermic CSTR when $\sigma = 2$ are represented in Figure 4.10.

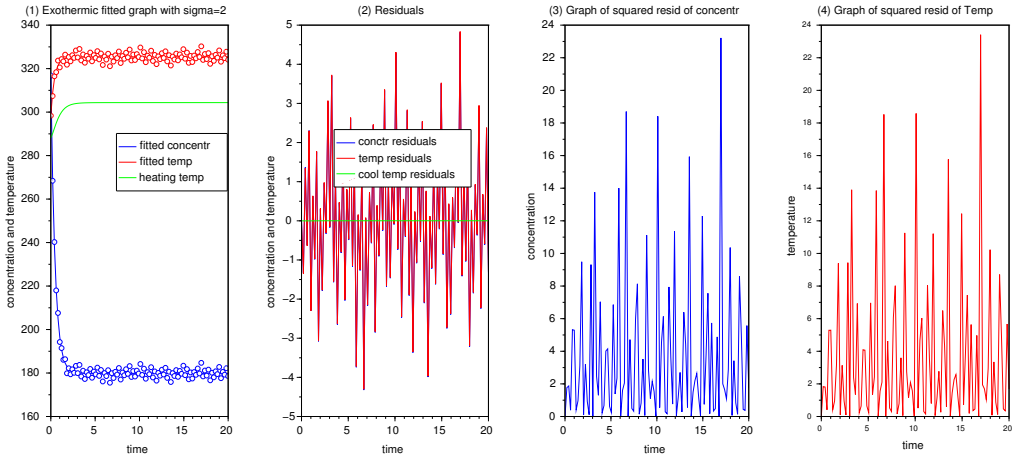

Figure 4.10: Plots showing the fitted curves of the exothermic CSTR model. Sub-plot (1) points out the fitted temperature and concentration. Sub-plot (2) represents the residuals while sub-plots (3) and (4) show the squared residuals of concentration and temperature respectively. The experimental parameters are $k = 0.9$, $E = 0.5$ and the estimated parameters become $k = 0.9006$, $E = -25.7933$.

As the previous case of the exothermic CSTR, the estimated parameters are computed using the fminsearch function in scilab. The obtained estimated reaction rate is greater than its experimental parameter but converges to its true value with the small difference of 0.0006. The estimated activation energy is negative and greater than its true value in absolute value. However, it is the closest result in absolute value obtained compared to the other results obtained in this research. To quantify how good the fit is in Figure 4.10, we based it on the variation of the residuals and the squared residuals of the components (variables) of the models. In sub-plot (2), the concentration and temperature residuals are located in a range of $[-4.5, 4.85]$, but more of them are accumulated in interval $[-1, 1]$. Therefore, not much deviation between observations and estimated values were observed. Again, the squared residuals of the concentration vary in the range of 0 and 23.2 with the mean value of 3.6297, while the squared residuals of the temperature vary in a range of $[0, 23.4]$ with the mean value of 3.63. The squared residuals of cooling temperature vary around zero with a negligible mean value of 0.0000020521 as it could not be seen on the squared residuals graph. A large number of data points among one hundred points fit the curves.

We next, repeat the same simulations but with a different levels of noise with $\sigma = 10$.

We start by the true solutions and quasi noisy solutions. The simulation results are as shown in Figure 4.11.

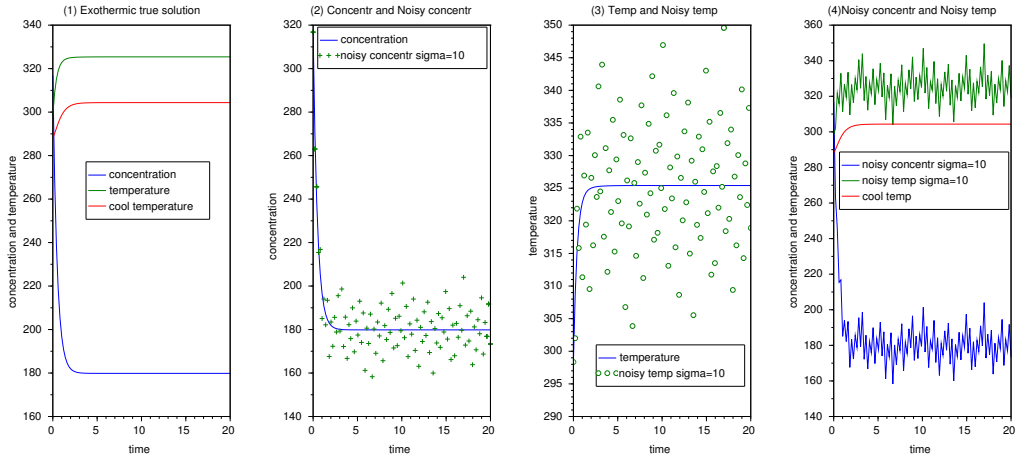

Figure 4.11: Graphs showing the numerical solutions and noisy solutions of exothermic CSTR. The type and level of noise is quasi with $\sigma = 10$. Sub-plot (1) shows the numerical solutions (true solutions), sub-plots (2) and (3) represent the concentration and temperature with quasi random noise respectively. Sub-plot (4) includes both numerical solutions and noisy solutions. The experimental parameters are $k = 0.9$ and $E = 0.5$.

The results show that quasi random noisy data points are spreading along the true solutions curves but in a highly correlated manner. The effect is high randomness in the numerical solutions compared to Figure 4.11.

We continue with the fitted curves and residuals graphs. The results are as shown in 4.12.

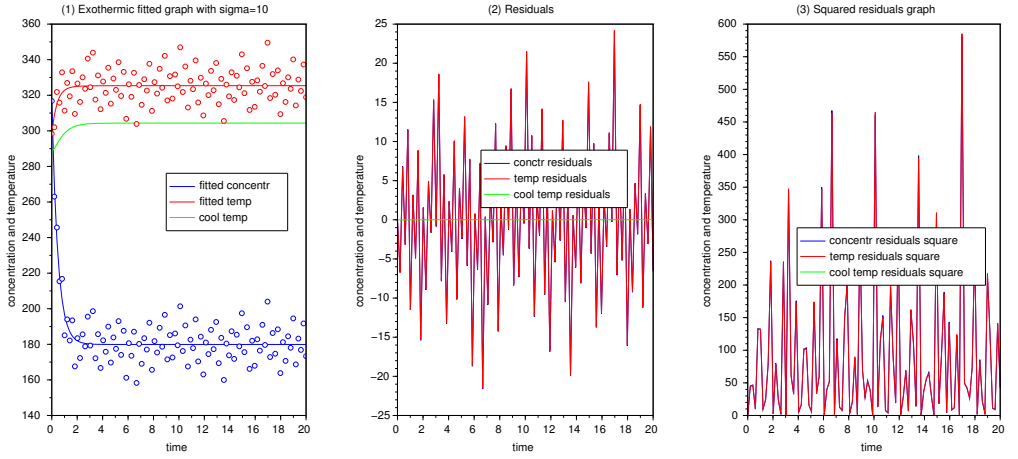

Figure 4.12: Graphs showing the fitted curves of exothermic CSTR model. Sub-plot (1) shows the fitted temperature and concentration. Sub-plot (2) represents the residuals while sub-plot (3) shows the squared residuals of concentration and temperature. The fixed parameters are $k = 0.9$, $E = 0.5$ and the estimated parameters become $k = 0.903$, $E = -131.54$. The noise level is determined by $\sigma = 10$.

From Figure 4.12, the simulations show that the reaction rate converges to its true value with the difference of 0.003 while the activation energy becomes high in the negative sense. The squared residuals of the concentration and temperature vary in intervals $[0, 580.4]$ and $[0, 585.3]$ with the mean values of 90.74 and 90.75 respectively, as seen in sub-plot (3). The squared residuals of the cooling temperature vary around 0 but with the mean value of 0.0000509, which cannot be seen on the squared residuals graph. The scale of residuals has increased from -22 to 24 with more of them between $[-5, 5]$. Therefore, the difference between the observations and the estimated values is large as may be viewed in Figure 4.12. As a consequence, a small number of data points among hundred fit the concentration and temperature curves.

4.2.2 Endothermic CSTR

Quasi random noise is again added to the concentration and temperature numerical solutions of CSTR with endothermic reactions to simulate and estimate its parameters. The added noise is of two types and two levels, one with small variance ($\sigma = 2$) and the other with big variance ($\sigma = 10$). We generated one hundred data points of this kind of noise using the R-code generator, due to the dimension of the iterations and the numerical solutions of the endothermic CSTR model, provided by odesolver. Again, the considered sequence of noise is called Sobol sequence, which is evenly distributed.

Starting with $\sigma = 2$, the numerical solutions and noisy solutions are as shown in Figure 4.13.

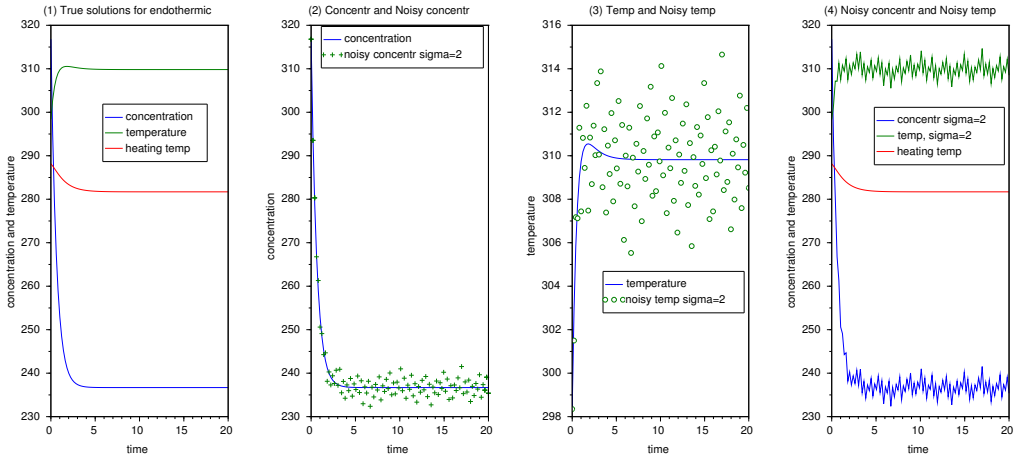

Figure 4.13: Graphs describing the numerical implementation of CSTR model with endothermic reactions. Sub-plot (1) gives overview of the true solutions whereas sub-plots (2), (3) and (4) show the noisy solutions. The true parameters are $k = 0.4$ and $E = 0.5$. The type of noise in data is quasi with $\sigma = 2$.

Figure 4.13 shows the numerical solutions, where the quasi random noisy solutions are distributed along both sides of the numerical solution curves of the endothermic CSTR, in a highly correlated manner. We observe the oblique drawn lines of noisy solutions as patterns on both side of sub-plots (2) and (3) in Figure 4.13.

The endothermic CSTR fitted curves, residuals graphs and its estimated parameters with $\sigma = 2$ are visualized in Figure 4.14.

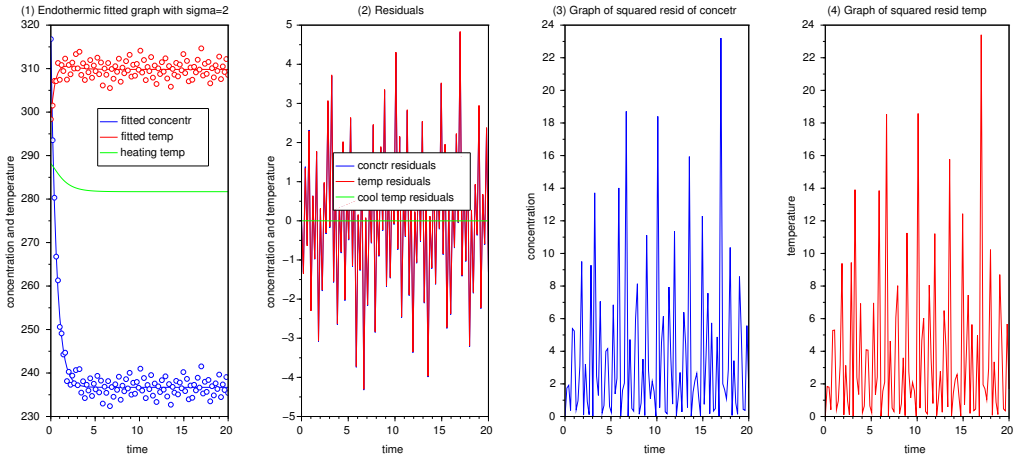

Figure 4.14: Graph (1) represents the model fitting, graph (2) represents the residuals, graphs (3) and (4) show the squared residuals of concentration and temperature respectively. Level of noise is $\sigma = 2$ and the experimental parameters involved in numerical simulations are $k = 0.4$ and $E = 0.5$. Estimated parameters from Minimization Assimilation method become $k = 0.4008$ and $E = -144.1007$.

The results show that, the reaction rate becomes large but convergent to its true parameter with the difference error of 0.0008 while the activation energy parameter is negative and diverges from its true value. Nevertheless, it is among the smallest values in absolute value compared to the activation energy values in absolute obtained in this work. The variation of the squared residuals of the concentration becomes $[0, 23.2]$ with the mean value of 3.629 while the squared residuals of the temperature vary between 0 and 23.4 with the mean value of 3.63. The squared residuals of the heating temperature cannot be seen on the graph of squared residuals since they are around zero with a negligible mean value of 0.00000077041. In sub-plot (2) of Figure 4.14, the residuals of the concentration and the temperature are spreading in the interval $[-4.5, 4.58]$, but more of them are accumulated around zero in a range $[-1, 1]$. This means the difference between the observations and the estimated values is not very significant. As a result, we observe at least good marginal fit of the data points to the model.

Proceeding with $\sigma = 10$, then the numerical solutions and noisy solutions are as seen in Figure 4.15.

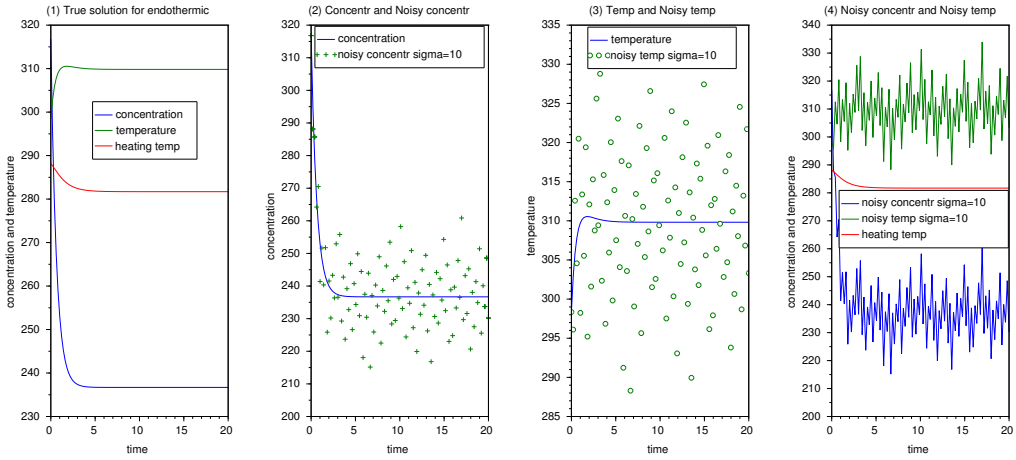

Figure 4.15: Graphs describing the numerical implementation of CSTR model with the endothermic reactions. Sub-plot (1) gives overview of the true solutions whereas sub-plots (2), (3) and (4) show the noisy solutions. The true parameters are $k = 0.4$ and $E = 0.5$. The type of noise in data is quasi with $\sigma = 10$.

We have remarked that quasi random noise covers a big space of the grid in a strong correlation as observed in Figure 4.15. This means the points are located far from the true curves, and could have an impact on model fitting and parameter estimation.

Figure 4.16 describes the fitted curves, the residuals' graphs and the estimated parameters for the endothermic CSTR when $\sigma = 10$.

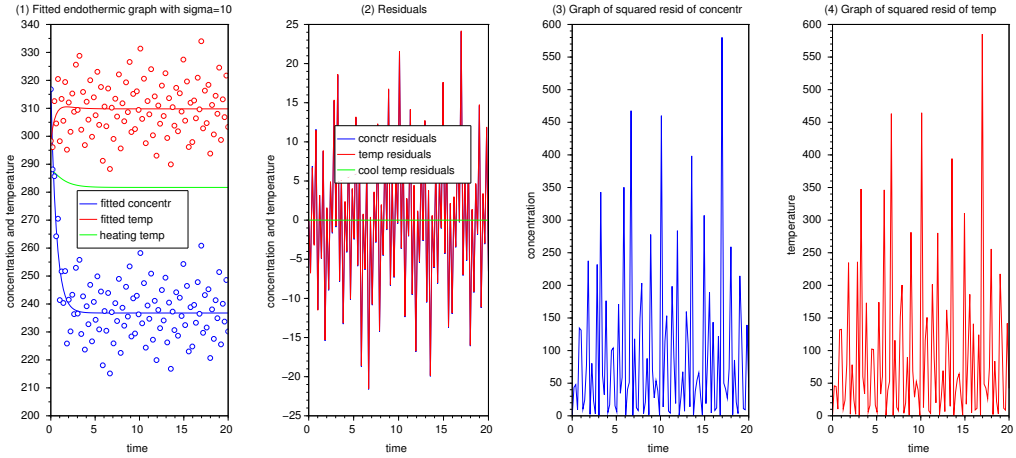

Figure 4.16: Graph (1) represents the model fitting, graph (2) represents the residuals, graphs (3) and (4) show the squared residuals of concentration and temperature respectively. Level of noise is $\sigma = 10$ and the experimental parameters involved in numerical simulations are $k = 0.4$ and $E = 0.5$. Estimated parameters from Minimization Assimilation method become $k = 0.4037$ and $E = -705.8411$.

It is clear that the values of the estimated activation energy has increased in the absolute value compared to the result obtained from Figure 4.14. However, the reaction rate converges to its true value with the difference error of 0.0037. The difference between the observations and the estimated solutions is significant as the concentration and temperature residuals vary between -22 and 24 with most of them accumulated in $[-5, 5]$. The variations of squared residuals of the concentration and temperature become $[0, 580.2]$ and $[0, 585.2]$ with the mean values of 90.7415 and 90.7572 respectively, and hence slightly increase. The mean value of the squared residuals of the heating temperature for this case is 0.00001911, which allows the squared residuals of the heating temperature to be around zero and negligible. Consequently, the data points do not fit the model well compared to the fitted curves in Figure 4.14. This is the negative impact of high variability in the numerical solutions caused by the increase of the quasi random noise.

4.3 Systematic Random Noise

Systematic random noise was added in the concentration and temperature numerical solutions of both CSTRs (with exothermic and endothermic reactions) in regards to generate systematic random data. This kind of data is of two types. The first type contains noise with a small standard deviation $(\sigma = 2)$ while the second noise data contains a big standard deviation $(\sigma = 10)$. We used this "cooked data" to simulate and estimate the parameters of CSTRs, which in turn gives the information about mismatch among the parameters and deviation of the data to the fitting models.

4.3.1 Exothermic CSTR

In this subsection, we are looking at the uncertainties in the model fitting and its influence on the model constructed, based on the exothermic reactions in a continuously stirred tank reactor. To proceed, we have to deal with the parameter estimation of the model, which are the reaction rate (k) and the activation energy (E). We have fixed the true parameters to be $k = 0.9$ and $E = 0.5$ for the first time, by generating the assumed true solutions (numerical solutions) for the exothermic system. After adding systematic random noise, generated using the scilab random generator, with standard deviation $\sigma = 2$, $\sigma = 10$ and mean $(\mu = 0)$ in the obtained concentration and the temperature numerical solutions, we were able to cook systematic noisy data. This data was taken as the measurements of the concentration and the temperature of the substance at time t, and helps to simulate and estimate the parameters of the process.

Similarly, Figure 4.17 represents the true solutions and the noisy solutions for exothermic CSTR model with systematic noise produced using $\sigma = 2$.

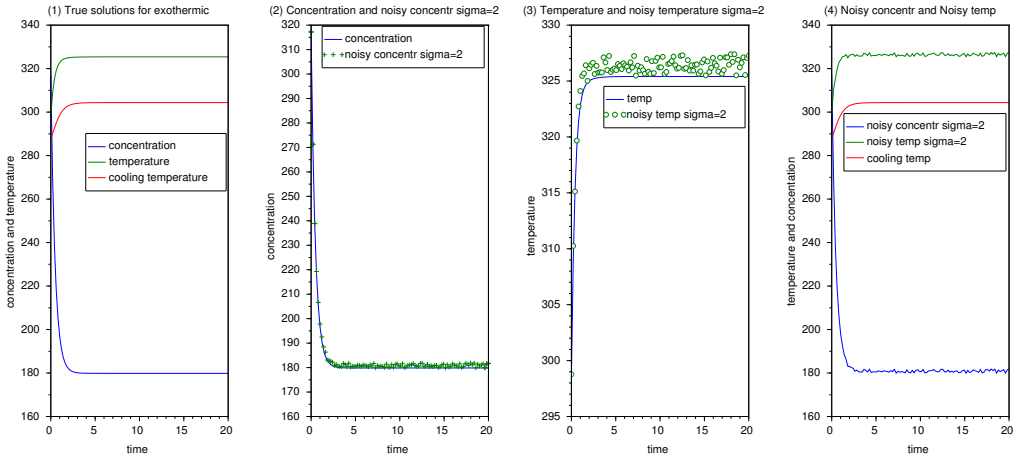

Figure 4.17: Graphs showing the numerical solutions and systematic noisy solutions of the exothermic CSTR model. Sub-plot (1) shows the true solutions while sub-plots (2), (3) and (4) represent the noisy solutions. The level of noise is given by $\sigma = 2$. The experimental parameters are $k = 0.9$ and $E = 0.5$.

In Figure 4.17, sub-plot (1) shows that concentration of the substance is decreasing from 316 with time and reaches its equilibrium state at 180 within $4s$. Also, it shows the cooling temperature that enters the process through the cooling jacket to regularize the process temperature. Since the coolant enters with the low temperature compared to the temperature of the process, then the coolant temperature increases automatically due to the heat transfer until both temperatures stabilize. Sub-plots (2), (3) and (4) point out the noisy solutions of the concentration and temperature. It is clear that the noise is systematic as it is located on the positive side of the concentration and temperature curves.

Figure 4.18 indicates the fitted exothermic CSTR models with systematic random noise produced by $\sigma = 2$, as well as the residuals graphs.

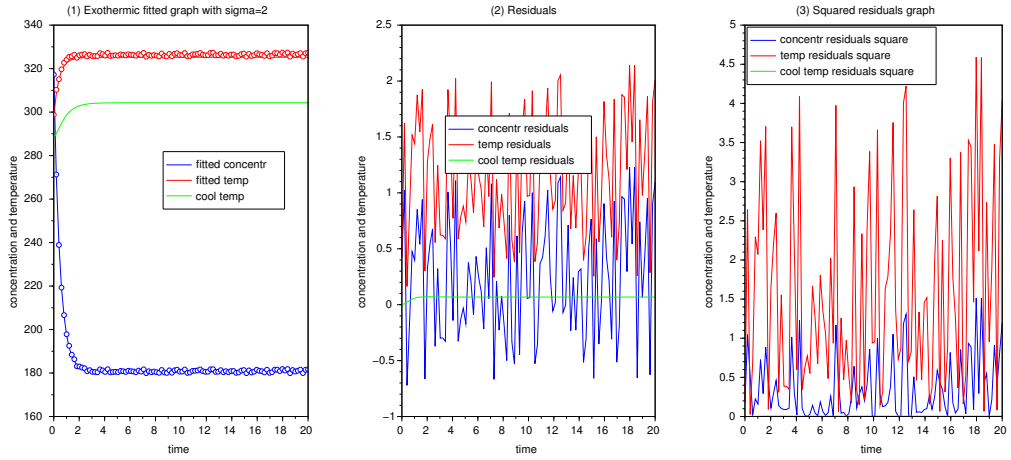

Figure 4.18: Graphs representing the fitted curves of exothermic CSTR model. Sub-plot (1) shows the fitting temperature and concentration curves. Sub-plots (2) and (3) respectively show the residuals and squared residuals. The true parameters involved are $k = 0.9$ and $E = 0.5$ and estimated parameters are $k = 0.8893$ and $E = 65.5958$. The level of systematic noise is determined by $\sigma = 2$.

The results show that the parameter for the activation energy does not converge to the true value. Nevertheless, it is the second among the smallest estimated activation energy values in this research. The reaction rate converges to the true parameter with the difference error of 0.0107. The concentration residuals are spreading in a range of $[-0.7, 1.2]$, but more among them are accumulated in $[-0.5, 0.5]$. On the other hand, the temperature residuals are varying in a range of $[0.2, 2.14]$ with a big number of them in the scale of $[0.5, 1.5]$. Therefore, small differences between concentrations, temperatures and their estimated values are experienced in a system. From sub-plot (3), the squared residuals of the concentration vary in the range $[0, 1.5146]$ with the mean value of 0.349 while the squared residuals of the temperature range from 0 up to 4.5929 with the mean value of 1.6231. The squared residuals for the cooling temperature are varying around zero with the mean value of 0.0045. As the residual values and their mean values are small, then, all hundred data points fit the model as it is shown in Figure 4.18.

The Figure 4.19 illustrates graphs of the true solutions and systematic noisy solutions of exothermic CSTR when $\sigma = 10$.

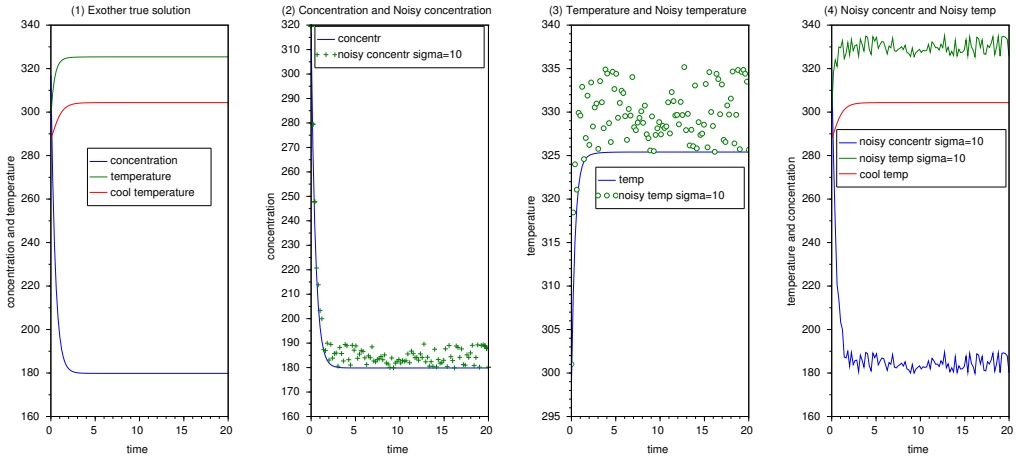

Figure 4.19: Graphs showing the numerical solutions and systematic noisy solutions of exothermic CSTR model. Sub-plot (1) shows the true solutions while sub-plots (2), (3) and (4) represent the noisy solutions. The level of noise is given by $\sigma = 10$. The experimental parameters are $k = 0.9$ and $E = 0.5$.

The result is the same as those in Figures 4.17 and 4.18, except that systematic randomness in data has increased due to large standard deviation. The same fitted and residual graphs but different standard deviation $\sigma = 10$, are shown in Figure 4.20.

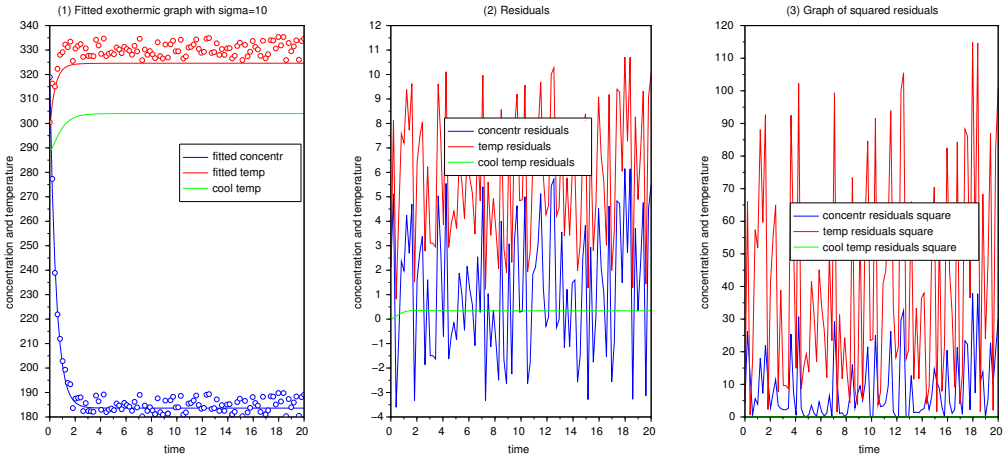

Figure 4.20: Graphs representing the fitted curves of exothermic CSTR model. Sub-plot (1) shows the fitting temperature and concentration curves. Sub-plots (2) and (3) respectively show the residuals and squared residuals. The true parameters involved are $k = 0.9$ and $E = 0.5$ and estimated parameters are $k = 0.847$ and $E = 364.97$. The level of systematic random noise is determined by $\sigma = 10$.

In Figure 4.20, the result shows that the activation energy becomes large compared to its true parameter, but the reaction rate seems to converge since the only difference from the true value is 0.053. From these estimated values, we can say that they become large compared to the results obtained in Figure

4.18. In sub-plot (1) of Figure 4.20, variability of noisy data increased in the fitting models. The scale of concentration residuals has increased from -3.5 to 6.15 with an accumulation of them in the range $[-2, 2]$ while the residuals of temperature increase the scale from 0 up to 10.7 with more accumulation in $[3, 8]$. Hence, the difference between the observations and the estimated values becomes big. From sub-plot (3), the squared residuals of concentration are varying in $[0, 37.878]$ with the mean value of 8.7 and the squared residuals of the temperature are varying in a range of $[0, 114.81]$ with the mean value of 40.6 while the squared residuals of the cooling temperature vary around zero with the mean value of 0.112. Hence, the mean values of the squared residuals for the concentration and the temperature have increased. Therefore, a large number of data points does not fit the model well.

4.3.2 Endothermic CSTR

This part gathers the simulations and the results obtained from the CSTR model equations, with the heating jacket. The same procedure applied to the exothermic will be considered in this subsection. The only differences were based on fixed parameters, the sign of enthalpy and the sign of the heat transfer term. For this case, the true parameters were $k = 0.4$ and $E = 0.5$. Therefore, the results from simulations are shown from Figure 4.21 to Figure 4.24.

We again, take two different levels of systematic random noise in the numerical solutions from the endothermic CSTR. The first case is when $\sigma = 2$ and the second case is when $\sigma = 10$.

For $\sigma = 2$, the numerical solutions and noisy solutions are as shown in Figure 4.21.

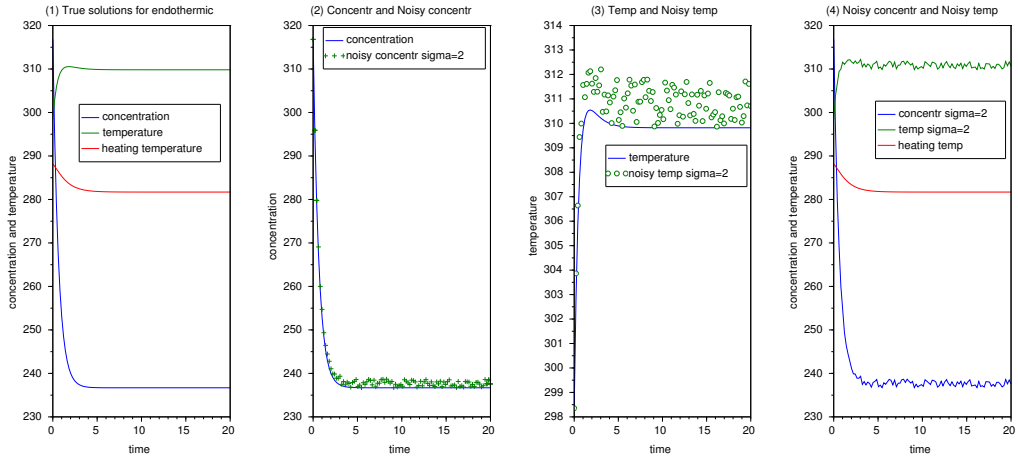

Figure 4.21: Graphs showing the numerical solutions and systematic noisy solutions of the endothermic CSTR. Sub-plot (1) represents the true solutions while sub-plots (2), (3) and (4) indicate systematic noisy solutions. The true parameters used are $k = 0.4$ and $E = 0.5$. Level of systematic random noise is given by $\sigma = 2$.

From Figure 4.21, sub-plot (1) shows the heating substance enters the the tank with a high temperature to trigger the reaction. After heating the substance at the lowest temperature in a reactor, the temperature of the reactor increases, while the heating temperature decreases until both temperatures reach their equilibrium states. Other sub-plots of Figure 4.21 correspond to the systematic noisy concentration and systematic noisy temperature solutions. In sub-plot (2), we have concentration with the

systematic noisy solution while in sub-plot (3), there is systematic noisy temperature solution. The noise is generated systematically in such a way that it is located on the positive side of the models.

For $\sigma = 2$ also, the fitted curves and residuals graphs are as show in Figure 4.22.

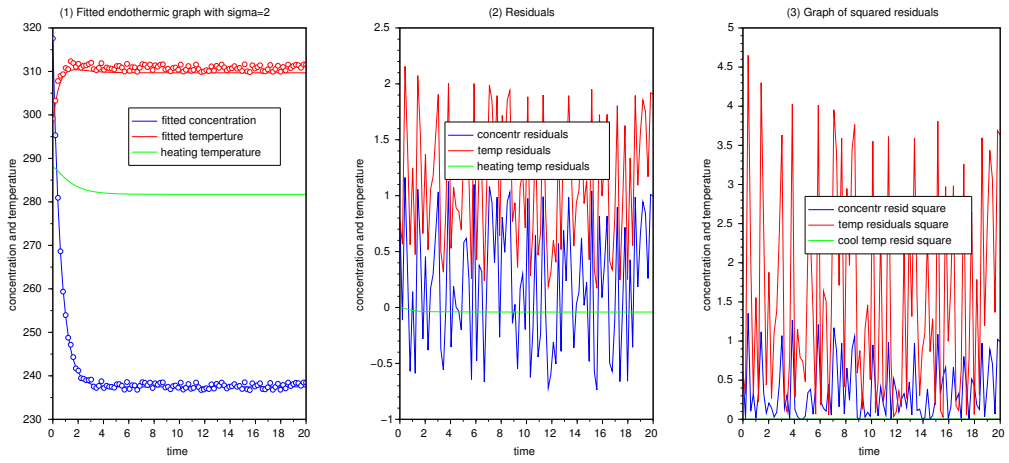

Figure 4.22: Graphs showing the fitted curves and residuals graph of endothermic CSTR model. Sub-plot (1) shows the fitted curves, sub-plots (2) and (3) represent the residuals and squared residuals respectively. In this case, the experimental parameters are $k = 0.4$ and $E = 0.5$ while the estimated parameters are $k = 0.388$ and $E = 1173$. Level of noise is given by $\sigma = 2$.

In Figure 4.22, the rate of reaction converges to the true parameter with the difference error of 0.012 but the activation energy diverges from its real value. In sub-plot (2), the concentration residuals are oscillating between -0.8 and 1.6 with much accumulation in a range of $[-0.5, 1]$ while the scale of the temperature residuals is varying in $[0.1, 2.1]$ with much accumulation in $[0.5, 1.9]$. Hence, there is no big difference between the observations (concentration and temperature) and their estimated values. The plot of squared residuals shows that the squared residuals of the concentration are varying in $[0, 1.35]$ with the mean value of 0.370099, while the squared residuals of temperature are varying in $[0, 4.65]$ with the mean value of 1.561065. The mean value of the squared residuals of the heating temperature becomes 0.0015, which is very small. As a result, the data points fit the model well.

Lastly, we show the effect of systematic random noise on the endothermic CSTR model when $\sigma = 10$.

when $\sigma = 10$, the numerical solutions and noisy solutions are as shown in Figure 4.24.

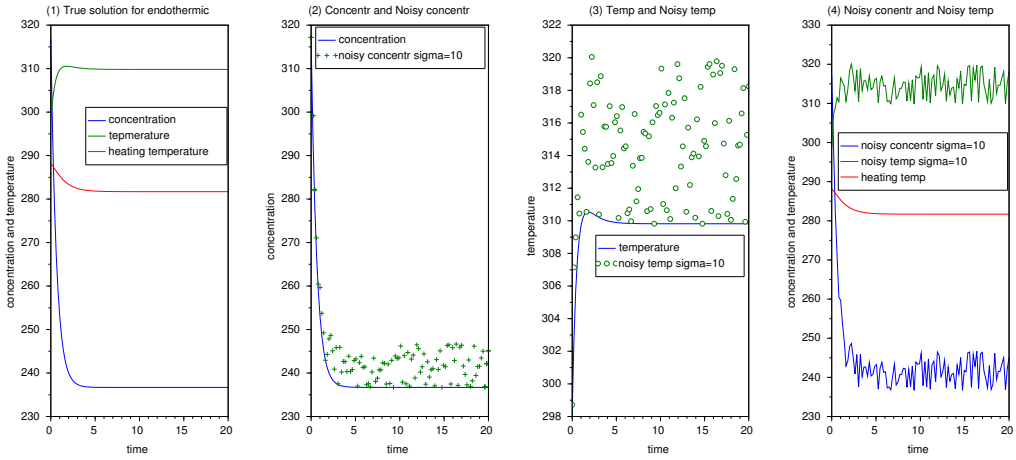

Figure 4.23: Graphs showing the numerical solutions and systematic noisy solutions of the endothermic CSTR. Sub-plot (1) represents the true solutions while sub-plots (2), (3) and (4) indicate systematic noisy solutions. The true parameters used are $k = 0.4$ and $E = 0.5$. Level of systematic random noise is given by $\sigma = 10$.

Variability in the systematic noisy solutions has increased on the positive side of the true solution curves compared to the corresponding sub-plots in Figure 4.21.

When $\sigma = 10$, the fitted curves and residual graphs of the endothermic CSTR model are as shown in Figure 4.24.

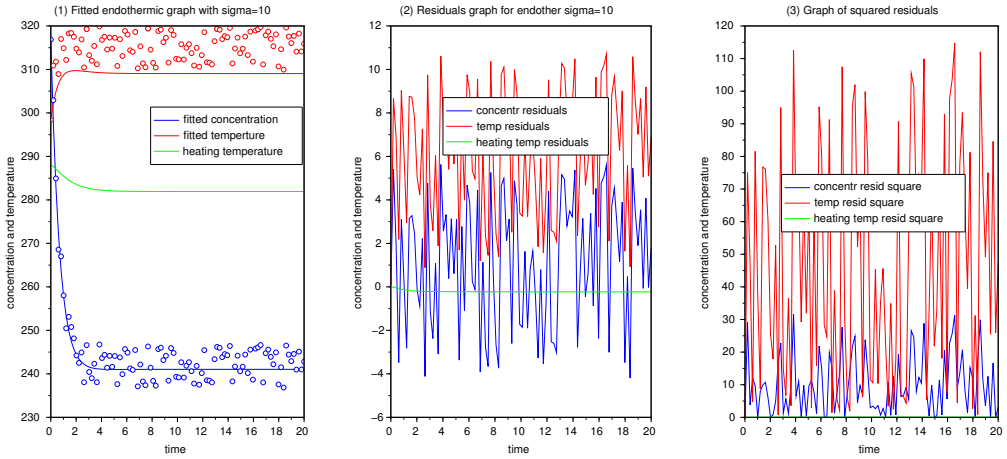

Figure 4.24: Graphs showing the fitted curves and residuals graph of the endothermic CSTR model. Sub-plot (1) shows the fitted curves, sub-plots (2) and (3) represent the residuals and squared residuals respectively. In this case, the experimental parameters are $k = 0.4$ and $E = 0.5$ while the estimated parameters become $k = 0.3442$ and $E = 5352.8$. Level of noise is given by $\sigma = 10$.

From Figure 4.24, the estimated activation energy E becomes very large, while the reaction rate param-

eter k has known deviation of 0.0558 from its true value. In sub-plot (2), the concentration residuals are oscillating in interval $[-4, 5.63]$, with more accumulation in a scale of $[-2, 3]$ while the temperature residuals are bounded in $[0.9, 10.73]$ with high accumulation in $[2, 9]$. Hence, most of the observations are different from the estimated values. Also, the squared residuals of the concentration are varying in a range of $[0, 31.7]$ with the mean value of 10.0174 whilst the squared residuals of the temperature are spreading in $[0, 115]$ with the mean value of 47.332562. The squared residuals of the heating temperature are oscillating around zero and its mean value becomes 0.0474. The range of residuals has increased and the squared residuals for concentration and reactor temperature have increased. The impact corresponds to much deviation in the model fitting as observed in Figure 4.24.

Table 4.2 shows summary of the results obtained in this work for each case and for each type and level of noise.

Table 4.2: Table of the Results

Exothermic CSTR	**Endothermic CSTR**
true parameters are $[k, E]$=[0.9, 0.5]	true parameters are $[k, E]$=[0.4, 0.5]
initials=[1, 1];[1,0.6];[0.8,0.4];[0.1,0.1];[0.9,0.5]	initials=[1, 1];[0.5,0.6];[0.3,0.4];[0.1,0.1];[0.4,0.5]
Random noise for $\sigma = 2$	**Random noise** for $\sigma = 2$
estimated are $k = 0.8853$ and $E = 377.2327$	estimated are $k = 0.3948$ and $E = 485.6932$
mean of squared resid of the concentr is 0.34584	mean of squared resid of the concentr is 0.3028747
mean of squared resid of the temp is 0.5917550	mean of squared resid of the temp is 0.5334537
mean of squared resid of the cooling temp is 0.00082698	mean of squared resid of the heating temp is 0.00029228
Random noise for $\sigma = 10$	**Random noise** for $\sigma = 10$
estimated are $k = 0.9044$ and $E = -129.39$	estimated are $k = 0.3782$ and $E = 3606.8183$
mean of squared resid of the concentr is 7.8652	mean of squared resid of the concentr is 7.7814381
mean of squared resid of the temp is 7.8723	mean of squared resid of temp is 7.8997289
mean of squared resid of the cooling temp is 0.000023	mean of squared resid of the heating temp is 0.000086324
Quasi random noise for $\sigma = 2$	**Quasi random noise** for $\sigma = 2$
estimated are $k = 0.9006$ and $E = -25.7933$	estimated $k = 0.4008$ and $E = -144.1007$
mean of squared resid of the concentr is 3.6297	mean of squared resid of the concentr is 3.6297
mean of squared resid of the temp is 3.6303	mean of squared resid of the temperature is 3.6303
mean of squared resid of the cooling temp is 0.0000020521	mean of squared resid of the heating temp is 0.00000077041
Quasi random noise for $\sigma = 10$	**Quasi random noise** for $\sigma = 10$
estimated are $k = 0.903$ and $E = -131.54$	estimated are $k = 0.4037$ and $E = -705.8411$
mean of squared resid of the concentr is 90.74	mean of squared resid of the concentr is 90.7415
mean of squared resid of the temp is 90.75	mean of squared resid of the temp is 90.7572
mean of squared resid of the cooling temp is 0.0000509	mean of squared resid of the heating temp is 0.000019111
Systematic random noise for $\sigma = 2$	**Systematic random noise** for $\sigma = 2$
estimated are $k = 0.8893$ and $E = 65.5958$	estimated are $k = 0.388$ and $E = 1173.0331$
mean of squared resid of the concentr is 0.349	mean of squared resid of the concentr is 0.370099
mean of squared resid of the temp is 1.6231	mean of squared resid of the temp is 1.561065
mean of squared resid of cooling temp is 0.0045	mean of squared resid of heating temp is 0.0015
Systematic random noise for $\sigma = 10$	**Systematic random noise** for $\sigma = 10$
estimated $k = 0.847$ and $E = 364.97$	estimated are $k = 0.3442$ and $E = 5352.8252$
mean of squared resid of the concentr is 8.7454	mean of squared resid of the concentr is 10.0174
mean of squared resid of the temp is 40.577	mean of squared resid of the temp is 47.332562
mean of squared resid of the cooling temp is 0.112	mean of squared resid of the heating temperature temp is 0.0474

5. Conclusion and Recommendation

In this project, numerical simulations and the parameter estimation of CSTRs based on exothermic and endothermic reactions have been discussed using the Minimization Assimilation method (Least squares method). We introduced three types of noise with different levels to the numerical solutions obtained by fixing true parameters, in order to generate six different kinds of data, taken as measurements of the continuously stirred tank reactors (exothermic and endothermic CSTRs) at time t. This noise data helped us to simulate and estimate the parameters, where the increase of noise into the system has an impact on the parameter estimation and the model fitting. The different true parameters were fixed to be $k = 0.9$ and $E = 0.5$ for the CSTR with exothermic reactions and $k = 0.4$, $E = 0.5$ for the CSTR with endothermic reactions and have been compared with their estimated parameter values.

The influence of noise on the parameter estimation and the fitting model for continuously stirred tank reactors was tracked, by observing the difference between the experimental parameter values and the estimated ones. The best fitting was determined by computing the variation of residuals, squared residuals and their mean values in the system. The smaller the variation and the mean values of residuals, the best fit the model. The results show that the Minimization Assimilation seems to fail to provide convergent activation energies though, the reaction rate converges. Moreover, the increase of noise into the system influences the activation energy more than the reaction rate. The activation energies of endothermic CSTR show the behaviour of being influenced by the noise more than the ones of exothermic CSTR. The fact that the method failed to provide convergent values for activation energy has not, to our knowledge, been explained as our system is not identifiable. The challenge we faced in this research is to test whether our estimated parameters are robust, since this one requires the exact and real data from any known system. Therefore, the loss of information may have resulted from guessing the parameters. Further work needs to be done on this challenge by using real measurements from the industries as the case of study to prove these parameters.

Acknowledgements

I would like first to thank the Almighty God for protecting and keeping me in good health during this period of the essay phase. I would also like to acknowledge the founder of AIMS and the AIMS Tanzania staff for helping me and making my life easy by providing everything during my academic year of study. My sincere gratitude goes to my supervisor Prof. Tuomo Kauranne and my co-supervisor Dr. Matylda Jablonska Sabuka for their amazing help and guidance to accomplish this work.

I am grateful and highly appreciate my tutors, especially, Dr. Pierre Yves for his help in the analysis part of this work, Mr. Babi for mentoring and correcting, Mrs. Elizabeth Horne for issues relating to english and Mr. Titus for issues relating to latex. Last but not least, many thanks goes to my family, friends and classmates for their motivation and inspiration during my studies.

References

S. Asprey and S. Macchietto. Statistical tools for optimal dynamic model building. *Computers and Chemical Engineering*, 24(2):1261–1267, 2000.

S. Asprey and S. Macchietto. Designing robust optimal dynamic experiments. *Journal of Process Control*, 12(4):545–556, 2002.

D. S. Bayard, R. Jelliffe, and M. Neely. Bayes risk as an alternative to fisher information in determining experimental designs for nonparametric models. In *Population Optimal Design of Experiments Workshop, Windlesham, Surrey, United Kingdom. http://www. maths. qmul. ac. uk/ bb/PODE/PODE2013_Slides/PODE2013_RogerJelliffe. pdf*, 2013.

P. Dostál, J. Vojtesek, and V. Bobál. Simulation of adaptive control of a continuous stirred tank reactor. In *ECMS*, pages 525–530, 2009.

M. A. Gandhi. Robust kalman filters using generalized maximum likelihood-type estimators. 2009.

H. Karimi. Parameter estimation techniques for nonlinear dynamic models with limited data, process disturbances and modeling errors. 2013.

P. Karkalousos and A. Evangelopoulos. *Quality control in clinical laboratories*. 2009.

T. Kauranne. Data assimilation. Class Notes. Retrieved from https://sites.google.com/a/aims.ac.tz/data-assimilation---2014/course-notes, Accessed in June, 2015.

S. Korkel, E. Kostina, H. G. Bock, and J. P. Schloder. Numerical methods for optimal control problems in design of robust optimal experiments for nonlinear dynamic processes. *Optimization Methods and Software*, 19(3-4):327–338, 2004.

N. R. Kristensen and H. Madsen. Continuous time stochastic modelling, ctsm 2.3-user's guide. *Technical University of Denmark, Lyngby, Denmark*, 2003.

I. S. Mbalawata et al. Adaptivemarkov chain monte carlo and bayesian filtering for state space models. *Acta Universitatis Lappeenrantaensis*, 2014.

B. G. Osorio, H. B. Castro, and J. D. S. Torres. State and unknown input estimation in a cstr using higher-order sliding mode observer. In *LARC*, pages 1–5, 2011.

D. Rosso. *Mass transfer at contaminated bubble interfaces*. PhD thesis, UNIVERSITY OF CALIFORNIA Los Angeles, 2005.

RPI, Accessed 2015. Continuous culture ,ideal cstr, cstr in series, and pfr. http://www.rpi.edu/dept/chem-eng/Biotech-Environ/Projects00/contin/project.htm, Accessed July, 2015.

S. Sahu. Multivariate adaptive regression spline based framework for statistically parsimonious adaptive dynamic programming. 2011.

D. Telen, D. Vercammen, F. Logist, and J. Van Impe. Robustifying optimal experiment design for nonlinear, dynamic (bio) chemical systems. *Computers & Chemical Engineering*, 71:415–425, 2014.

M. S. Varziri, K. B. McAuley, and P. J. McLellan. Approximate maximum likelihood parameter estimation for nonlinear dynamic models: Application to a laboratory-scale nylon reactor model. *Industrial & Engineering Chemistry Research*, 47(19):7274–7283, 2008.

J. Vojtesek and P. Dostal. Simulation analyses of continuous stirred tank reactor. In *Proceedings of the 22nd European Conference on Modelling and Simulation*, pages 506–511, 2008.

J. Voros, J. Miklevs, and L. vCirka. Parameter estimation of nonlinear systems. *Acta Chimica Slovaca*, 1(1):309–320, 2008.

M. Willis. Continuous stirred tank reactor models. *Dept. of Chemical and Process Engineering, University of Newcastle*, 2000.